

A Wearable Hand Assistive Device

Project report submitted in partial fulfillment of the requirements for the award of the
degree of

BACHELOR OF TECHNOLOGY
in
MECHANICAL ENGINEERING

by

Nilesh Balu
ME20B121

Under the guidance of

Prof. Manish Anand



Department of Mechanical Engineering
INDIAN INSTITUTE OF TECHNOLOGY MADRAS

19th May 2024

DECLARATION

I certify that the ideas, designs, experimental work, results, analyses, and conclusions presented in this dissertation are entirely my own effort, except where otherwise indicated and acknowledged. Furthermore, I affirm that the work is original and has not been previously submitted for assessment in any other course or institution unless explicitly stated otherwise.

A handwritten signature in blue ink, appearing to read "nileshbalu", is written over a dotted line.

Nilesh Balu

Roll No.: ME20B121

Date: Sunday 19th May, 2024

Place: Chennai 600 036

CERTIFICATE

This is to certify that the project report titled, “A Wearable Hand Assistive Device”, submitted by Nilesh Balu, ME20B121, to the Indian Institute of Technology Madras for the award of the degree of Bachelor of Technology in Mechanical Engineering, is a bonafide record of the project work carried out by him under my supervision. The contents of this report, whether in full or in part, have not been submitted to any other institute or university for the award of any degree or diploma.



Prof. Manish Anand

Professor

Department of Mechanical Engineering
Indian Institute of Technology Madras

Date: Friday 17th May, 2024

Place: Chennai 600 036

Prof. Chandramouli, P.

Head of the Department

Department of Mechanical Engineering
Indian Institute of Technology Madras

Date: Friday 17th May, 2024

Place: Chennai 600 036

ACKNOWLEDGEMENTS

Firstly, I would like to thank Prof. Manish Anand, Design Section, Department of Mechanical Engineering, for his guidance and support throughout this project. His assistance and dedication to supervising this project allowed me to gain a greater understanding of the technical aspects of design, product development, and control. I am forever grateful for the learnings I attained while working under him.

Secondly, I would like to thank the members of the BioNEx lab for their invaluable support during this project. Interactions with the scholars and engineers have been enriching, providing me with valuable insights. Their guidance and collaborative spirit have greatly influenced the direction and outcomes of my project.

ABSTRACT

This project presents the proof of concept (POC) prototype of a wearable hand assistive device aimed at addressing the challenges faced by individuals with partial paralysis of the hand. The primary challenge faced by such individuals is the compromised motor control of their hands, which hinders their ability to carry out activities of daily living. This assistive device provides the necessary forces for users to grasp objects, enabling them to perform these routine tasks with greater independence. The device consists of three single-occupancy compartments for the thumb, index finger, and middle finger. The ring finger and little finger are housed together in a double-occupancy compartment. One DC motor actuates each compartment by employing an under-actuated tendon mechanism. Using this mechanism, the three independent degrees of freedom of each compartment are brought about using one actuator. Extension is brought about passively using elastic elements. This mechanism reduces the net number of actuators, thereby reducing the weight of the device. Using tendons instead of linkages further reduces the bulk and makes the device compliant, thereby increasing user comfort. All four compartments will have flexion-extension movement, while the thumb will have an extra degree of freedom for retroposition-opposition movements, enhancing its grasp versatility. Simulations and calculations are presented to compute the motor torque required to produce the necessary pinching force. Once the open-loop control prototype was established, force sensors and flex sensors were installed to close the control loop. This way, the device maintains a pre-determined force while grasping an object. The current POC prototype can make two gripping actions: cylindrical grasp and lateral pinch.

LIMITATIONS OF USE

The Department of Mechanical Engineering, IIT Madras, and the staff of IIT Madras, do not accept any responsibility for the truth, accuracy, or completeness of material contained within or associated with this dissertation.

Persons using all or any part of this material do so at their own risk, and not at the risk of the Department of Mechanical Engineering, IIT Madras, and the staff of IIT Madras.

This document, the associated hardware, software, drawings, and other material set out in the associated appendices should not be used for any other purpose: if they are so used, it is entirely at the risk of the user.

TABLE OF CONTENTS

ACKNOWLEDGEMENTS	iii
ABSTRACT	iv
LIMITATIONS OF USE	v
TABLE OF CONTENTS	vi
LIST OF FIGURES	viii
LIST OF TABLES	x
1 INTRODUCTION	1
1.1 Background	1
1.2 Literature Review	2
1.2.1 Introduction	2
1.2.2 Compliant Hand Exoskeletons	2
1.2.3 Patents	3
1.3 Present Study	3
2 THE MECHANICAL MODULE	5
2.1 Under-actuated Tendon Mechanism	5
2.2 Calculations	6
2.2.1 Tension and angle of attachment (θ)	6
2.2.2 Joint Angles and String Lengths	8
2.2.3 Modeling the flexion movement of the finger	9
2.3 Simulations	12

2.3.1	Motion of the links	12
2.3.2	Torque requirements	12
3	THE ELECTRONIC MODULE	16
3.1	Components used	16
3.1.1	Teensy 4.1 Development Board	16
3.1.2	L298N Dual Motor Driver	16
3.1.3	Spectra Symbol Flex Sensors	17
3.1.4	Robodo SEN37 Force Sensor Resistors	17
3.1.5	DC Motors	17
3.1.6	Advance Technologies EMG Muscle Sensor V3.0	17
3.2	The Setup	18
3.2.1	Testing Base - 3D Printed Hand	18
3.2.2	Calibration of the Flex Sensors	19
3.2.3	Calibration of Force Sensing Resistor	20
3.2.4	Calibration of EMG Sensors	21
3.2.5	Circuit Diagram	22
3.3	Placement of the EMG Sensors	27
3.4	Control levels	28
3.4.1	Grasp modes	28
3.4.2	State machines	29
3.4.3	Low-level control	32
4	RESULTS AND DISCUSSION	33
4.1	The prototype	33
4.2	Limitations and Future Work	35

LIST OF FIGURES

2.1.1 Routing of the cable	6
2.2.1 FBD: Tension vs Angle	7
2.2.2 Tension with varying θ	7
2.2.3 Angle vs String Length	8
2.2.4 Finger modeled as a Serial Linkage	9
2.2.5 FBD of the links	11
2.3.1 Grasping Motion	12
2.3.2 Simulation: Orientation 1	13
2.3.3 Simulation: Orientation 2	13
2.3.4 Block Diagram of each link in the index finger	14
2.3.5 Block Diagram of the Index Finger Model	14
2.3.6 Block Diagram of the Closed Loop System	15
3.2.1 The 3D printed hand	19
3.2.2 Flex Sensor Readings	20
3.2.3 Calibration of the FSR	21
3.2.4 EMG Sensor Readings: Flexor Group	22
3.2.5 EMG Sensor Readings: Extensor Group	22
3.2.6 Hand gestures and placement of electrodes	23
3.2.7 Components of the circuit	23
3.2.8 Components of the circuit continued	24
3.2.9 Circuit Diagram: Actuator Connections	25
3.2.10 Circuit Diagram: Sensor Connections	26
3.3.1 The Finger Flexor Group Source: Adapted from [17]	27

3.4.1 State Machine Diagram	31
4.1.1 Sensor glove	33
4.1.2 Actuation glove	34
4.1.3 Control System of the Prototype	34
4.1.4 Glove attached to the splint	35
4.1.5 Grasping a cylindrical object	35

LIST OF TABLES

3.1 Description of the state machine	31
--	----

CHAPTER 1

INTRODUCTION

1.1 Background

Spinal Cord Injuries (SCIs) are a very broad class of injuries in which the spinal cord is damaged due to traumatic injury or pathology associated with the spine. As of 2012, around 1.5 million people in India live with SCI, with 200,000 cases added every year [1]. The spinal cord is a bundle of nerves that connects the brain to the rest of the body. Depending on the exact location of the damage, the consequences of the injury will vary.

Partial paralysis often leads to a loss of motor skills, severely hindering an individual's ability to perform activities of daily living. In addition, many individuals face muscle pain and spasticity in their hands. Such individuals often depend on their caregivers to perform activities of daily living, like flipping a switch, using a remote, and drinking water from a bottle. This lack of independence could lead to a loss of self-esteem and can increase their frustration and anxiety.

A hand-assistive device could significantly improve their quality of life. Such a device would provide the necessary assistive forces required by the individual to grasp objects and carry out activities of daily living. With the aid of such a device, individuals would experience greater independence and confidence in managing their daily tasks.

1.2 Literature Review

1.2.1 Introduction

Hand exoskeletons have been in existence since the 1990's. Brown et al. in [2] proposed a solution where rigid links were coupled with a tendon mechanism to flex the fingers. This represented the flavor of most of the traditional exoskeletons, like the ones proposed by Rotella et al. in [3] and Martinez et al. in [4], wherein rigid links were used to actuate the fingers. These mechanisms, however, had the drawback of making the hand exoskeleton bulky, thereby leading to reduced user acceptance. In the past decade, researchers have been focusing on developing soft and compliant solutions to overcome this issue.

1.2.2 Compliant Hand Exoskeletons

Polygerinos et al. in [5] proposed a soft device wherein elastomeric bladders are pressurized using air to actuate the fingers. This solution was much lighter than the previous traditional solutions available at the time. Yap et al. in [6] developed an improved version of the pneumatically activated glove by adding corrugations to one side of the bladder and strain-limiting fabric on the other side. Their device also incorporated an open loop sEMG control system to detect the intent of the user. Yap et al. improved their mechanism by decreasing the weight of the device. Their work defined new criteria for the weight of hand assistive devices, viz., "the weight of the glove should be < 200 g, and the weight of the control system should be < 1.5 kg" [7].

Pneumatic actuators bring with them a few drawbacks. Firstly, it requires a compressor, which is fairly bulky and noisy. Further, pneumatic systems are prone to leakages, potentially leading to an increased number of maintenance checks. An under-actuated tendon mechanism serves as an alternative compliant solution that overcomes this issue. In et al. proposed such a mechanism in [8], along with a differential mechanism to actuate multiple fingers simultaneously with one actuator. Xiloyannis et al. in [9] developed a device that used one motor to actuate 8 DOFs of the hand, ensuring that the forces are distributed appropriately. Gerez et al. in [10] used EMG sensors to actuate the motors based on muscle

activity.

Chen et al. in [11] proposed a rehabilitation system where a glove with actuators mirrors the gestures made by a second glove fitted with force and flexion sensors. A potential improvement to the previous solutions proposed by researchers could be using sensors to get information about the state of the hand, thereby improving the functionality.

1.2.3 Patents

Ciocarlic and Stein in [12] patented a wearable hand orthotic that brings about the flexion of fingers using one motor or linear actuator and a network of tendons. This device used an EMG armband to detect user intention. Bugtai et al. in [13] presented a rehabilitation device that provides both passive and active flexion of individual fingers and the wrist. The motors used in this device are housed on the glove itself.

1.3 Present Study

One problem that requires addressing is incorporating multiple DOFs of the thumb in the same device. Another potential issue is the lack of a closed-loop control system to maintain a particular force while grasping objects. There are very few commercial products in the market that provide assistance to people with functional impairment of the hand. These are either rehabilitation devices or devices that deal with only grasp functionalities. There is a need to develop a device that offers independent control of the digits of the hand by detecting the intent of the user while still prioritizing low weight.

A wearable hand assistive device has been proposed in this thesis to address these issues. The device is compliant and uses an under-actuated tendon mechanism to bring about flexion of the digits of the hand. This device has a minimalist design, prioritizing weight reduction, simplicity, and low form factor. Force sensors and flex sensors, similar to the ones used in [11], are used in the glove to close the system, thereby making it more stable and reliable. Further, it offers independent actuation of all compartments in the device, including multiple

DOFs of the thumb. The POC prototype is capable of making 2 gestures at the moment: *cylindrical grasp* and *lateral pinch*. The device also makes use of EMG signals to detect the intent of the user, similar to [6].

CHAPTER 2

THE MECHANICAL MODULE

2.1 Under-actuated Tendon Mechanism

The human hand is really complex and has 27 DOFs [14]. The index finger of the hand, for instance, has 3 bones, namely, the *distal phalange*, *intermediate phalange* and *proximal phalange*. The *proximal phalange* is connected to a bone in the palm, called the *metacarpal*. Hence, the finger has 4 DOFs at the three joints, one at the *distal interphalangeal (DIP)*, one at the *proximal interphalangeal (PIP)* and two at the *metacarpophalangeal (MCP)*. The human hand also has tendons attached to these fingers on the palmar and dorsal side, running across the palm to the forearm. Contracting the tendons causes the links of the finger to move, either flex or extend. The middle, ring and little fingers also have similar underlying mechanisms and DOFs. The thumb, however, only has the distal and proximal phalanges. However, the thumb has a total of 5 DOFs. One at the interphalangeal joint, two at the MCP and two at the *carpometacarpal* joint.

In order to create a wearable assistive device, it is imperative to actuate these fingers in a manner similar to how the human hand works. If we were to control each DOF independently, then we would have to attach actuators like motors at each of the joints. This would make the device incredibly heavy and bulky. To bypass this problem, we use a much simpler under-actuated tendon mechanism. In this mechanism, one end of a string is attached to the distal link of the finger, and another end is attached to a motor. When the motor is actuated, the string pulls the distal end of the finger and causes the whole finger to flex.

While grasping objects, this mechanism would cause the finger to conform to the shape of the object that is being grasped, much like the human hand. In this manner, three actuators are reduced to just one. The proposed routing pattern is presented in Fig. 2.1.1

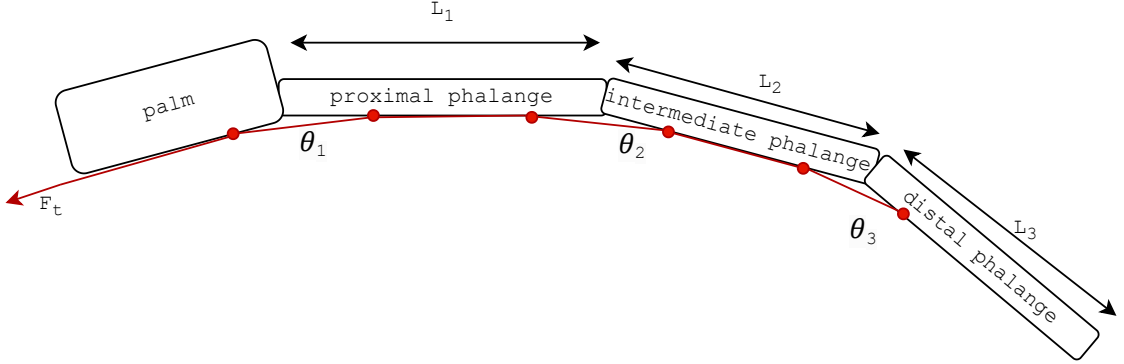


Figure 2.1.1: Routing of the cable

2.2 Calculations

2.2.1 Tension and angle of attachment (θ)

Calculations are conducted on one finger to compute the motor torque required to produce the required pinching force of 10 N. For this, a finger was modeled with three links that are in equilibrium with each other. Static force analysis was then performed.

$$\Sigma F_x = 0 \implies -F_t \cos(\beta - \theta) + R_x + F_c \sin \beta = 0$$

$$\Sigma F_y = 0 \implies R_y + F_c \cos \beta + F_t \sin(\beta - \theta) = 0$$

$$\Sigma M_C = 0 \implies F_c b - F_t \sin \theta a = 0$$

Solving these, we get the tension as a function of θ and F_c .

$$F_t = \frac{F_c b}{a \sin \theta}$$

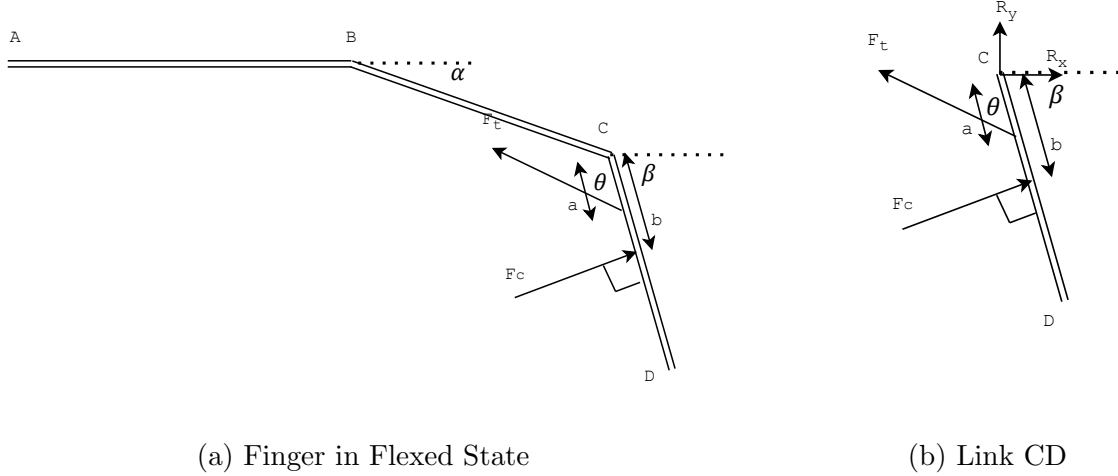


Figure 2.2.1: FBD: Tension vs Angle

From the above result it is clear that F_t is inversely proportional to a and $\sin\theta$. Thus, as the angle between the distal link and the cable increases, F_t decreases. This is shown in Fig. 2.2.2

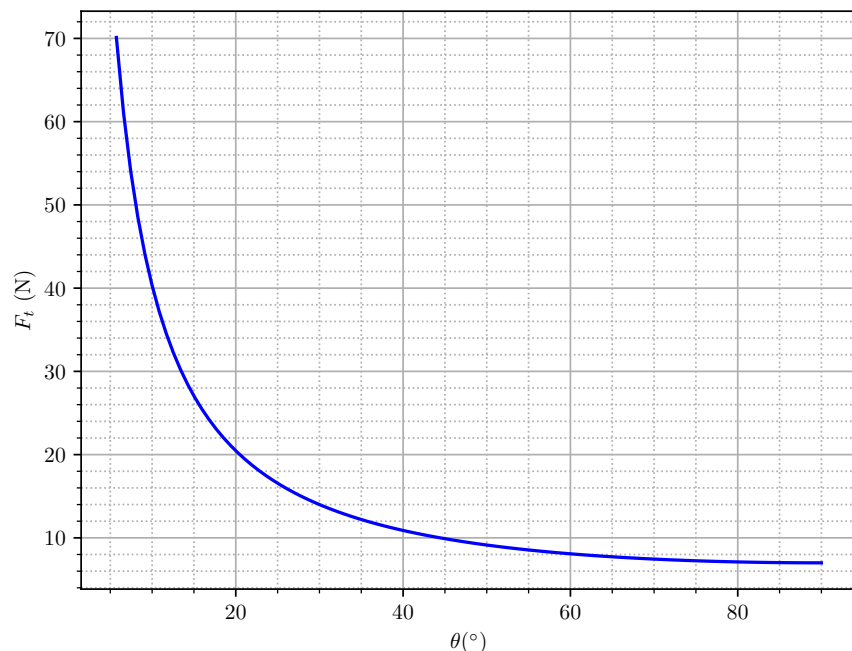


Figure 2.2.2: Tension with varying θ

2.2.2 Joint Angles and String Lengths

$$\Delta l = \Delta l_1 + \Delta l_2 + \Delta l_3$$

$$\theta_1 = f(\Delta l_1)$$

$$\theta_2 = f(\Delta l_2)$$

$$\theta_3 = f(\Delta l_3)$$

For a givens set of joint stiffness and assuming that there are no contact forces, there is a one-to-one mapping between $(\Delta l_1, \Delta l_2, \Delta l_3)$ and Δl .

Let a,b,c and d be design parameters as shown in the diagram.

$$\Delta l_i^2 = (b + c\cos\theta_i - d\sin\theta_1)^2 + (a - c\sin\theta_i - d\cos\theta_i)^2$$

Thus, we have obtained the function

$$\Delta l_i = \sqrt{(b + c\cos\theta_i - d\sin\theta_1)^2 + (a - c\sin\theta_i - d\cos\theta_i)^2}$$

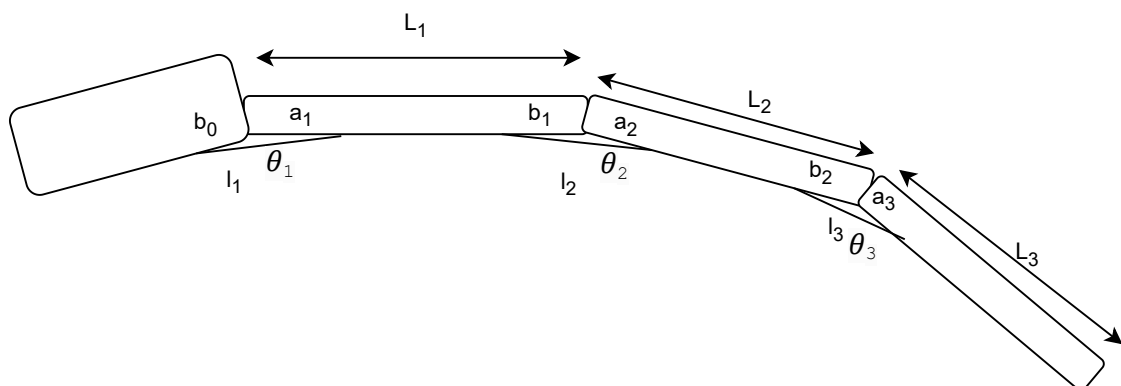


Figure 2.2.3: Angle vs String Length

$$l_1 = \sqrt{a_1^2 + b_0^2 - 2a_1b_0\cos\theta_1}$$

$$l_2 = \sqrt{a_2^2 + b_1^2 - 2a_2b_1\cos\theta_2}$$

$$l_3 = \sqrt{a_3^2 + b_2^2 - 2a_3b_2\cos\theta_3}$$

$$l = l_1 + l_2 + l_3 \rightarrow \text{net length of the string}$$

2.2.3 Modeling the flexion movement of the finger

Since the finger has been modeled as 3 rigid links attached in series, the accelerations at different points are related in the following manner:

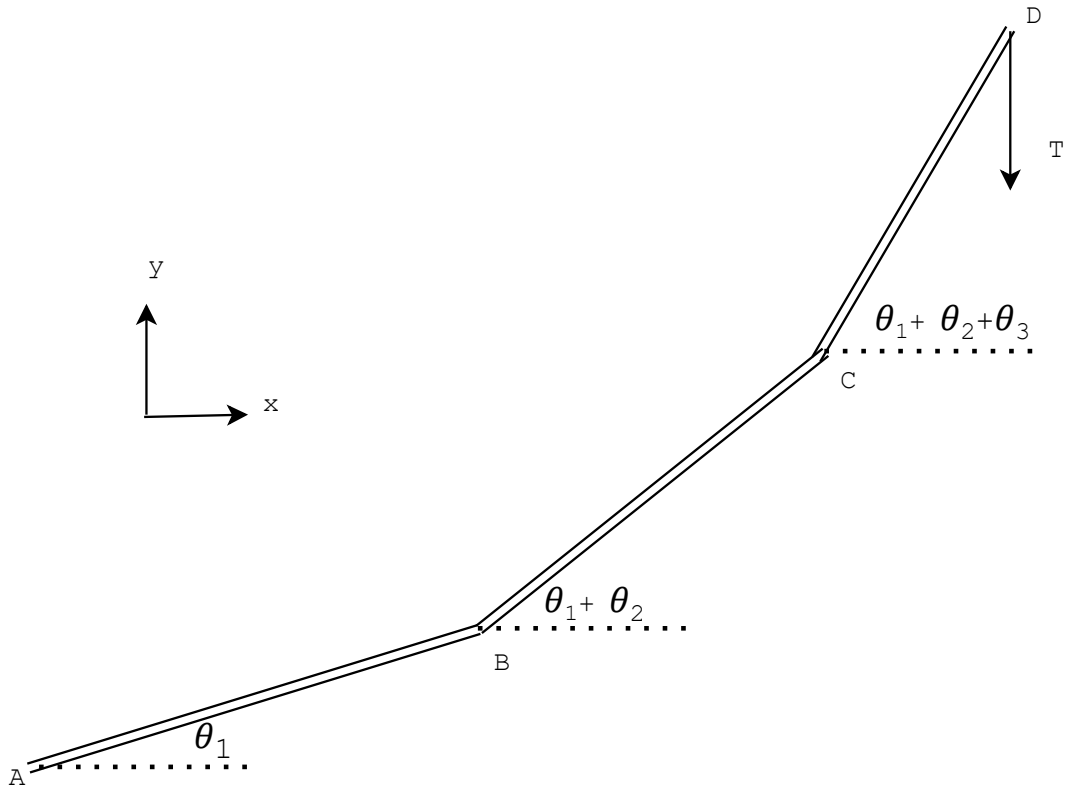


Figure 2.2.4: Finger modeled as a Serial Linkage

$$\begin{aligned}
a_{1x} &= \frac{-\alpha_1 l_1}{2} \sin \theta_1 - \frac{\omega_1^2 l_1}{2} \cos \theta_1 \\
a_{1y} &= \frac{\alpha_1 l_1}{2} \cos \theta_1 - \frac{\omega_1^2 l_1}{2} \sin \theta_1 \\
a_{Bx} &= -\alpha_1 l_1 \sin \theta_1 - \omega_1^2 l_1 \cos \theta_1 \\
a_{By} &= -\alpha_1 l_1 \cos \theta_1 - \omega_1^2 l_1 \sin \theta_1 \\
a_{2x} &= a_{Bx} - \frac{\alpha_2 l_2}{2} \sin(\theta_1 + \theta_2) - \frac{\omega_2^2 l_2}{2} \cos(\theta_1 + \theta_2) \\
a_{2y} &= a_{By} + \frac{\alpha_2 l_2}{2} \cos(\theta_1 + \theta_2) - \frac{\omega_2^2 l_2}{2} \sin(\theta_1 + \theta_2) \\
a_{Cx} &= a_{Bx} - \alpha_2 l_2 \sin(\theta_1 + \theta_2) - \omega_2^2 l_2 \cos(\theta_1 + \theta_2) \\
a_{Cy} &= a_{By} + \alpha_2 l_2 \cos(\theta_1 + \theta_2) - \omega_2^2 l_2 \sin(\theta_1 + \theta_2) \\
a_{3x} &= a_{Cx} - \frac{\alpha_3 l_3}{2} \sin(\theta_1 + \theta_2 + \theta_3) - \frac{\omega_3^2 l_3}{2} \cos(\theta_1 + \theta_2 + \theta_3) \\
a_{3y} &= a_{Cy} + \frac{\alpha_3 l_3}{2} \cos(\theta_1 + \theta_2 + \theta_3) - \frac{\omega_3^2 l_3}{2} \sin(\theta_1 + \theta_2 + \theta_3)
\end{aligned}$$

Using the above relations, we can write the equations of motion. The FBDs are given in Fig.

2.2.5.

$$\begin{aligned}
m_1 a_{1x} &= R_{Ax} - R_{Bx} - T \cos(\theta_1 - \alpha_1) + T \cos(\theta_1 + \beta_1) \\
\implies R_{Ax} &= m_1 a_{1x} + R_{Bx} + T \cos(\theta_1 - \alpha_1) - T \cos(\theta_1 + \beta_1) \\
m_1 a_{1y} &= R_{Ay} - R_{By} - T \sin(\theta_1 - \alpha_1) + T \sin(\theta_1 + \beta_1) \\
\implies R_{Ay} &= m_1 a_{1y} + R_{By} + T \sin(\theta_1 - \alpha_1) - T \sin(\theta_1 + \beta_1) \\
I_1 \alpha_1 &= R_{Bx} \frac{l_1}{2} \sin \theta_1 - R_{By} \frac{l}{2} \cos \theta_1 - R_{Ay} \frac{l_1}{2} \cos \theta_1 + R_{Ax} \frac{l_1}{2} \sin \theta_1 \\
&\quad - T \cos(\theta_1 - \alpha_1) \left(\frac{l_1}{2} - a_1 \right) \sin \theta_1 - T \cos(\theta_1 + \beta_1) \left(\frac{l_1}{2} - b_1 \right) \sin \theta_1
\end{aligned}$$

$$R_{Bx} = m_2 a_{2x} + R_{Cx} + T \cos(\theta_1 + \theta_2 - \alpha_1)$$

$$R_{By} = m_2 a_{2y} + R_{Cy} + T \sin(\theta_1 + \theta_2 - \alpha_1)$$

$$\begin{aligned} I_2 \alpha_2 &= (R_{Cx} \frac{l_2}{2} \sin(\theta_1 + \theta_2) - R_{Cy} \frac{l_2}{2} \cos(\theta_1 + \theta_2) - R_{By} \frac{l_2}{2} \cos(\theta_1 + \theta_2) \\ &\quad + R_{Bx} \frac{l_2}{2} \sin(\theta_1 + \theta_2) - T \cos(\theta_1 + \theta_2 - \alpha_2) (\frac{l_2}{2} - a_2) \sin(\theta_1 + \theta_2) \\ &\quad - T \cos(\theta_1 + \theta_2 + \beta_2) (\frac{l_2}{2} - b_2) \sin(\theta_1 + \theta_2) \\ &\quad + T \sin(\theta_1 + \theta_2 - \alpha_2) (\frac{l_2}{2} - a_2) \cos(\theta_1 + \theta_2) \\ &\quad + T \sin(\theta_1 + \theta_2 + \beta_2) (\frac{l_2}{2} - b_2) \cos(\theta_1 + \theta_2)) \end{aligned}$$

$$R_{Cx} = m_3 a_{3x} + T \cos(\theta_1 + \theta_2 + \theta_3 - \alpha_3)$$

$$R_{Cy} = m_3 a_{3y} + T \sin(\theta_1 + \theta_2 + \theta_3 - \alpha_3)$$

$$\begin{aligned} I_3 \alpha_3 &= R_{Cx} \frac{l_3}{2} \sin(\theta_1 + \theta_2 + \theta_3) - R_{Cy} \frac{l_3}{2} \cos(\theta_1 + \theta_2 + \theta_3) \\ &\quad - T \cos(\theta_1 + \theta_2 + \theta_3 - \alpha_3) (\frac{l_3}{2} - a_3) \sin(\theta_1 + \theta_2 + \theta_3) \\ &\quad + T \sin(\theta_1 + \theta_2 + \theta_3 - \alpha_3) (\frac{l_3}{2} - a_3) \cos(\theta_1 + \theta_2 + \theta_3) \end{aligned}$$

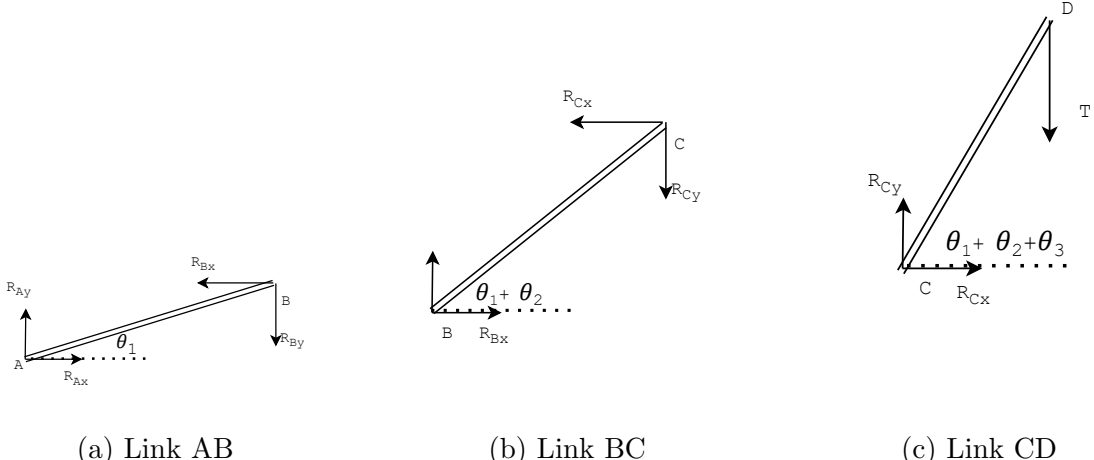


Figure 2.2.5: FBD of the links

These equations can then be passed into an ODE solver, like the *ode45()* solver on Matlab to simulate the motion of the underactuated mechanism.

2.3 Simulations

The under-actuated mechanism was modeled and simulated on *Simulink Multibody* [15]. In this manner, the calculations conducted prior to this were verified. Additionally, this enabled us to determine the optimal routing of the cable through the fingers.

2.3.1 Motion of the links

Firstly, a model was developed to simulate the motion of one finger. Each link of the finger was modeled to be a cuboid of appropriate length. This was primarily done to develop an intuition as to how the under-actuated tendon mechanism would actuate the links of the finger. Fig. 2.3.1 presents screenshots of the orientation of the fingers at different time instances.

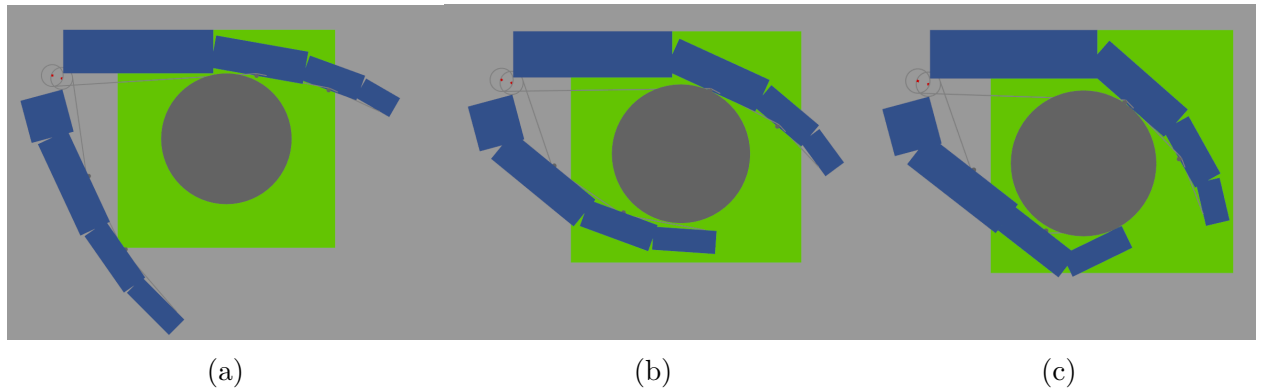
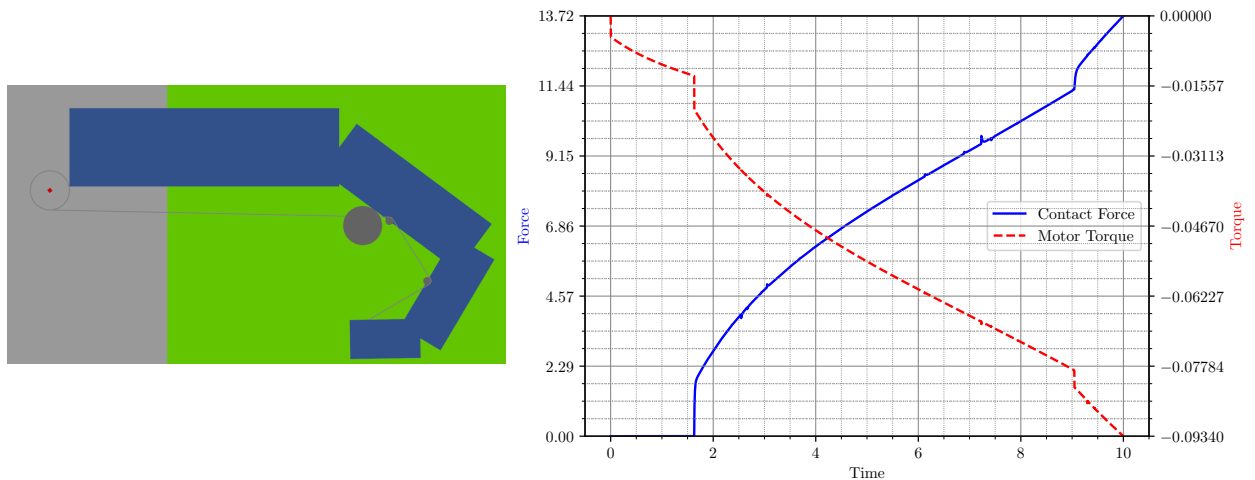


Figure 2.3.1: Grasping Motion

2.3.2 Torque requirements

Next, the simulations were carried out to compute the motor torque required to produce a pre-defined contact force. This was performed at different orientations, shown in Fig. 2.3.2 and Fig. 2.3.3, and was compared to the analytical calculations presented in the previous section.

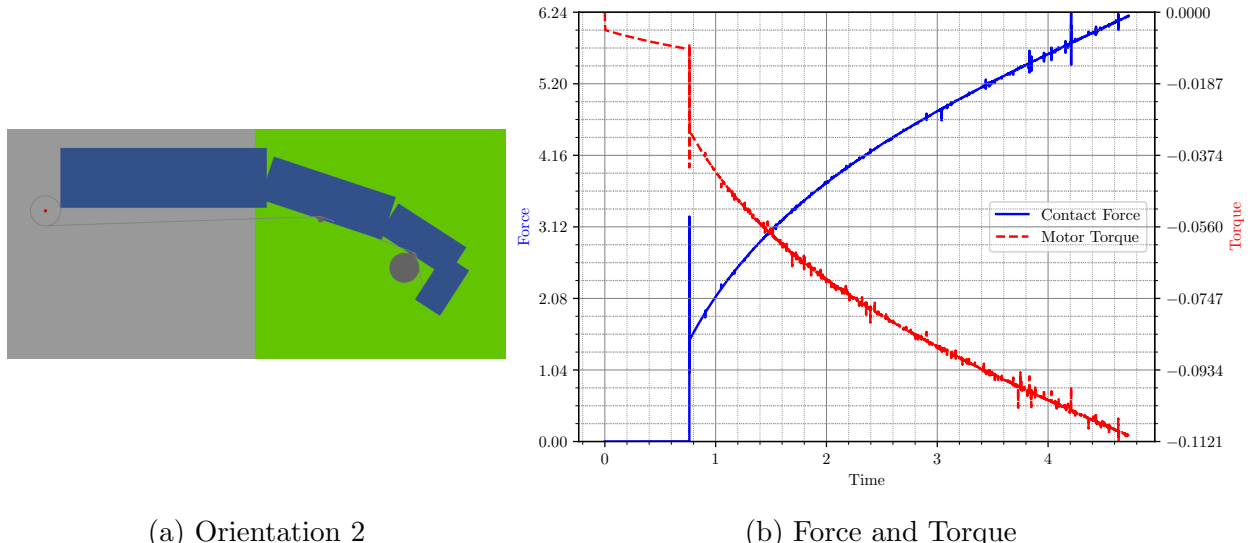
Fig. 2.3.6 depicts the Simulink block diagram that describes the simulation premise of the simulation done to calculate the forces required to produce a grip force of 20 N. The winds in the cable gradually and the contact force and torque are compared. Fig. 2.3.5 and Fig.



(a) Orientation 1

(b) Force and Torque

Figure 2.3.2: Simulation: Orientation 1



(a) Orientation 2

(b) Force and Torque

Figure 2.3.3: Simulation: Orientation 2

2.3.4 are inner layers of the block diagram.

From Fig. 2.3.2a and Fig. 2.3.3a, it is observed that at the time of grasping, $\theta = 45^\circ$. From Fig. 2.2.2, the required amount of tension in the cable in this orientation is 10 N. Thus, we need to choose a motor that is capable of providing a tension of 10 N on the cable.

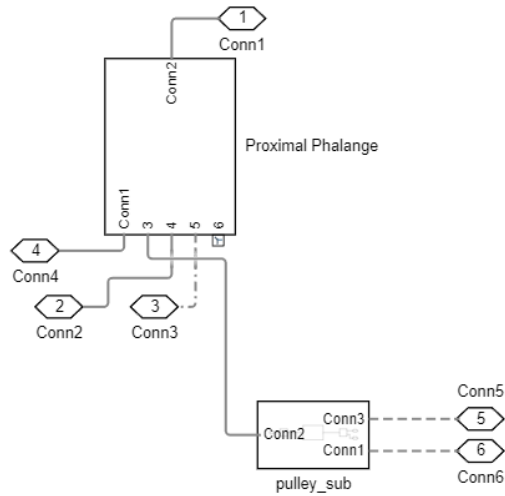


Figure 2.3.4: Block Diagram of each link in the index finger

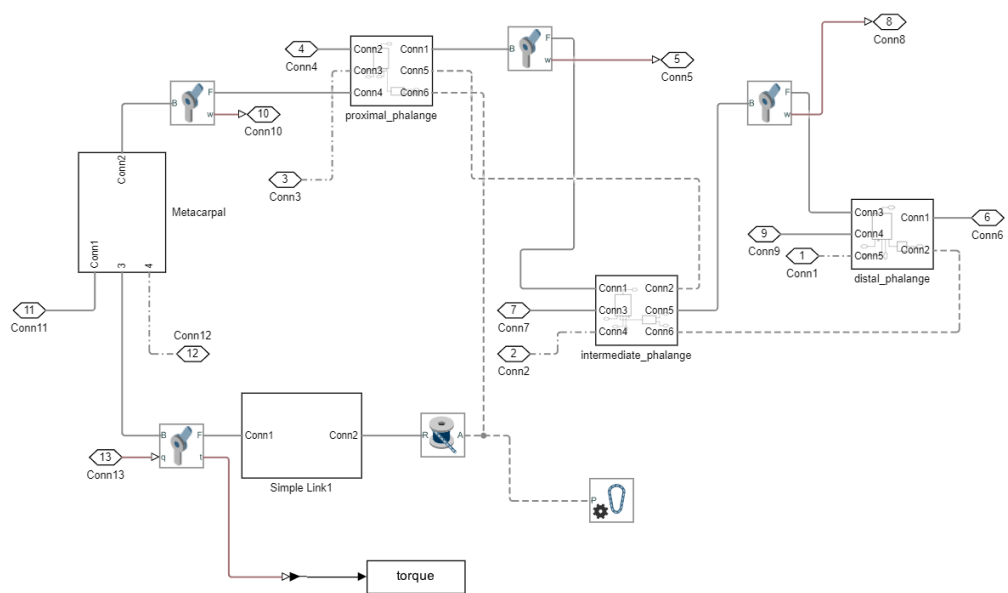


Figure 2.3.5: Block Diagram of the Index Finger Model

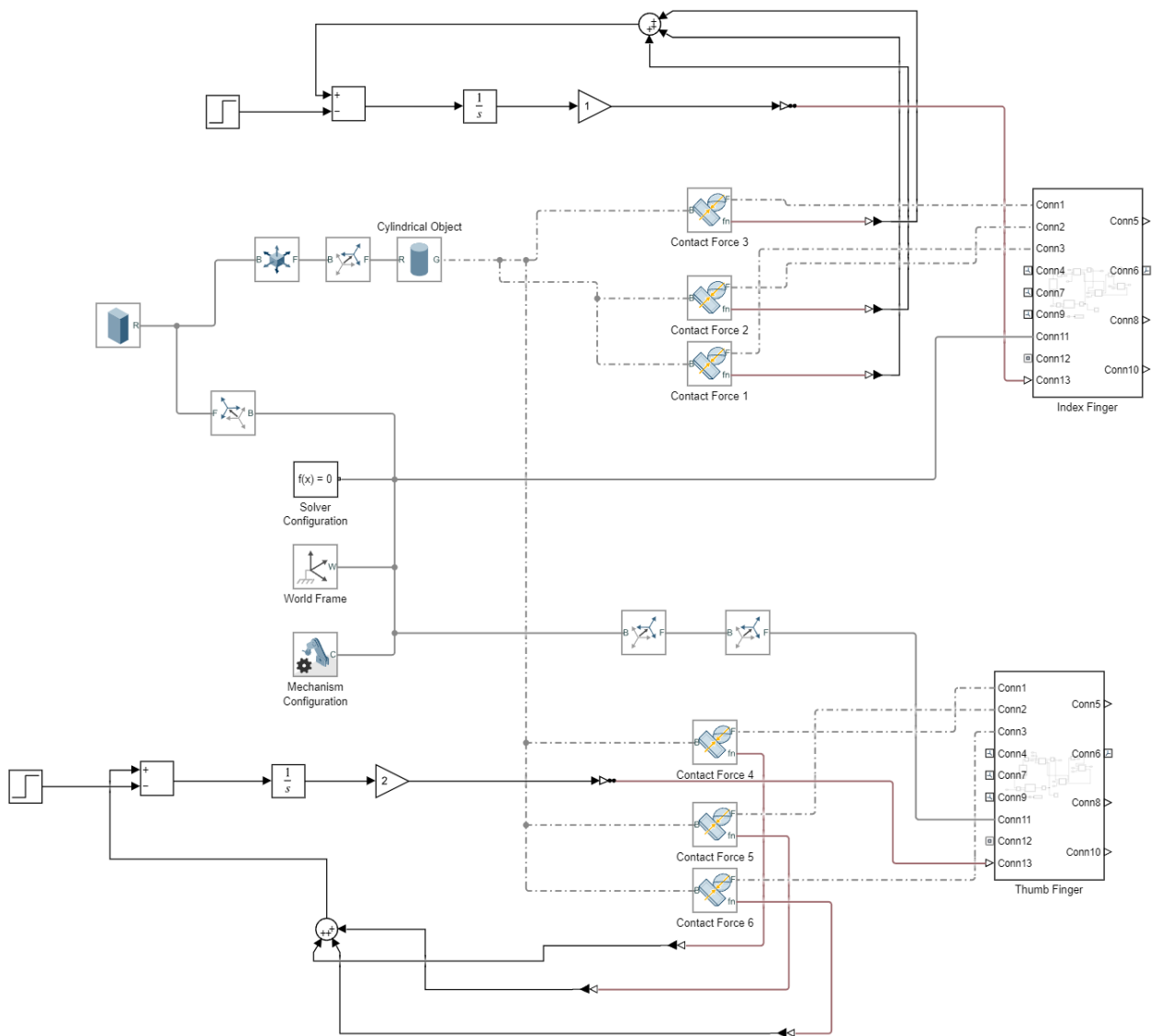


Figure 2.3.6: Block Diagram of the Closed Loop System

CHAPTER 3

THE ELECTRONIC MODULE

3.1 Components used

The following off-the-shelf electronic components were used in the prototype:

1. Teensy 4.1 Development Board
2. L298 Dual Motor Drivers
3. Spectra Symbol Flex Sensors
4. Robodo SEN37 Force Sensor Resistors
5. DC Motors
6. Advance Technologies EMG Muscle Sensor V3.0

3.1.1 Teensy 4.1 Development Board

The Teensy 4.1 chip houses an ARM Cortex-M7 processor. The primary reason for choosing the Teensy 4.1 as the microcontroller was the presence of over 40 General Purpose Input Output (GPIO) pins. This was necessary to connect all the required sensors housed in all compartments.

3.1.2 L298N Dual Motor Driver

The L298N motor driver controls the speed of the motor using PWM (Pulse Width Modulation) signals. In this way, the average power transmitted to the motor varies, in spite

of keeping the potential difference across the motors constant at 12 V. Changing the duty cycle of the PWM signal will change the power transmitted. In addition to this, the motor driver houses a h-bridge, which provides a means to change the direction of the motors. The L298N can control two DC motors simultaneously.

3.1.3 Spectra Symbol Flex Sensors

A flex sensor is used to measure the angle of deflection of the surface on which it is housed. It does this with the help of a conductive ink filled inside a segmented conductor [16]. The sensor is designed in such a way that the resistance changes linearly with the angle of bend. These sensors are useful to define the limits of flexion and extension, thereby acting as "limit switches".

3.1.4 Robodo SEN37 Force Sensor Resistors

These force-sensing resistors are used to measure the contact forces at the fingertips. Similar to flex sensors, there is a conductive material that reduces its resistance when force is applied to the surface of the sensor. This sensor is useful to close the control loop of the system.

3.1.5 DC Motors

The Xcluma Metal TT motor was used in this device. It has a maximum torque rating of 0.8 kg-cm. Attaching this to a spool of radius 8 mm gives a maximum tension of 9.8 N. This force, accompanied with good grip, should be sufficient to grasp objects.

3.1.6 Advance Technologies EMG Muscle Sensor V3.0

The EMG sensors are used to detect the user's intention. This sensor consists of three electrodes that are placed at different points on the forearm of the user. Two electrodes are on the flexor muscle group responsible for flexing the fingers and wrist. The third electrode is placed on a bony part of the arm for a reference potential. The two electrodes placed on the muscle group will measure the potential difference generated along the muscle group

when the muscles contract. This potential is usually very small and needs to be amplified to higher voltages. This is taken care of by the muscle sensor, which has an amplifying circuit.

3D printed components: Apart from electronic components, the following components were 3D printed:

1. A motor base to house each motor
2. A spool to wind and unwind the cable
3. Casing for the custom proto-board

Miscellaneous components: The other miscellaneous components used are:

1. A splint to house all the motor bases, controllers, and drivers
2. Fishing line as the cable - can withstand tensile forces up to 50 kgf
3. The glove

3.2 The Setup

3.2.1 Testing Base - 3D Printed Hand

The final product is a glove with strings attached to it. Testing the device on a healthy hand would lead to entirely subject inferences. And it would be both - dangerous and unethical to test it on a partially paralyzed hand. Hence, it made sense to create a testing setup that would provide a standard way to test the device and would enable us to track its progress by observing its improvement in a more objective fashion. For this purpose, a hand was 3D printed. Each link of the hand was printed separately, and the links were assembled together using implicitly defined press-fit revolute and ball-and-socket joints. This 3D-printed hand replicated the motion of the human hand sufficiently enough that it served as a good test setup. The glove is donned on the 3D-printed hand in the images provided in this report.

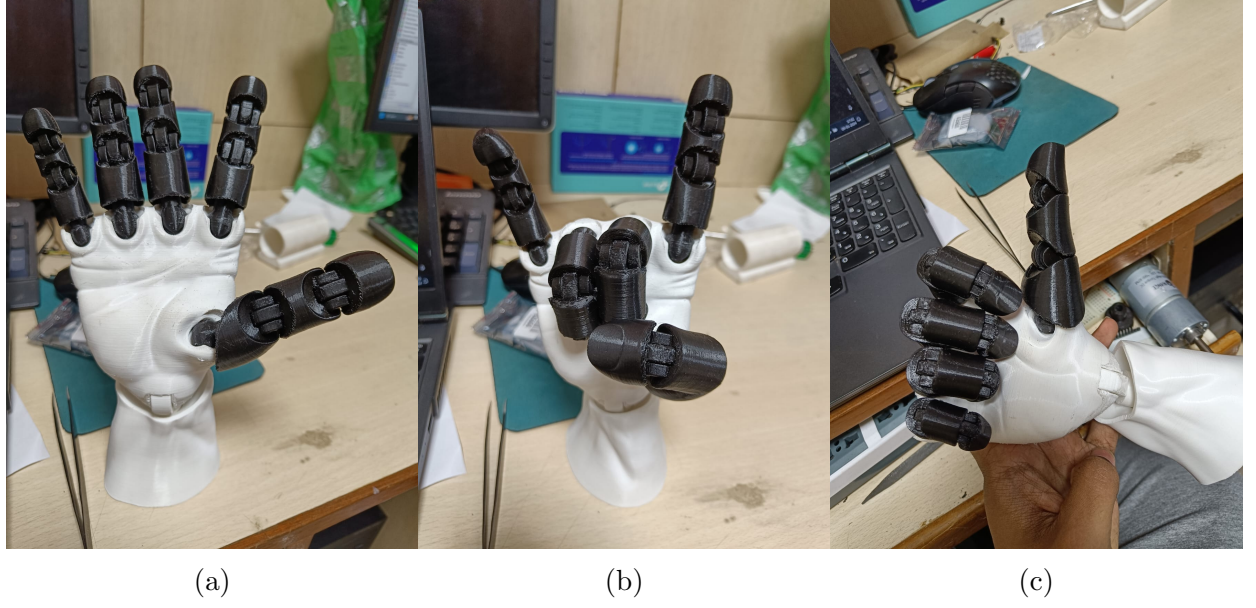


Figure 3.2.1: The 3D printed hand

3.2.2 Calibration of the Flex Sensors

Each flex sensor was calibrated independently. The resistances of the sensor were noted for $\theta = 0^\circ$ and $\theta = 90^\circ$ and the microcontroller was programmed to linearly interpolate between the two known resistances to find the angle of the sensor.

$$\theta \text{ (in }^\circ\text{)} = \frac{R_{\text{flex}} - R_0}{R_{90} - R_0} 90$$

where the resistance of the flex sensor is measured using a voltage divider using the 3v3 pin, the ground pin, and an analog pin in the microcontroller. The reference resistor is taken to be $R_b = 10k\Omega$

$$V_{\text{pin}} = \left(\frac{R_b}{R_b + R_{\text{flex}}} \right) V_{3.3}$$

$$\implies R_{\text{flex}} = R_b \left(\frac{V_{3.3}}{V_{\text{pin}}} - 1 \right)$$

The values corresponding to 0° and 90° are plotted in Fig. 3.2.2

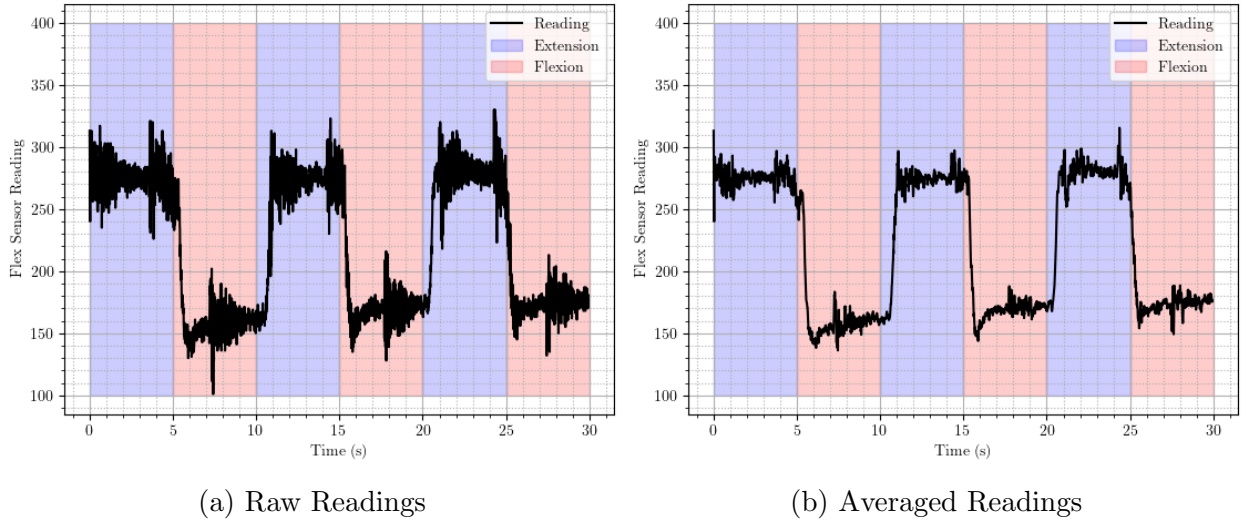


Figure 3.2.2: Flex Sensor Readings

3.2.3 Calibration of Force Sensing Resistor

The calibration of the FSRs is not as trivial. Calibration weights are used to measure the sensor readings at different inputs. The flex sensor is designed in such a way that $\log_{10}F$ and $\log_{10}R$ have a linear relationship.

$$\log_{10}(F) = a \log_{10}(R_{\text{fsr}}) + b$$

A curve of this form is fit on the data points measured for different weights. Using this fit curve, we get the measured force to be:

$$F = (R_{\text{fsr}})^a e^b$$

Again, the resistance of the FSR is measured using a voltage divider using the microcontroller pins.

$$V_{\text{pin}} = \left(\frac{R_b}{R_b + R_{\text{fsr}}} \right) V_{3.3}$$

$$\implies R_{\text{fsr}} = R_b \left(\frac{V_{3.3}}{V_{\text{pin}}} - 1 \right)$$

Calibration weights are used to calibrate the FSR. R_{fsr} is plotted against the weight and is presented in Fig. 3.2.3.

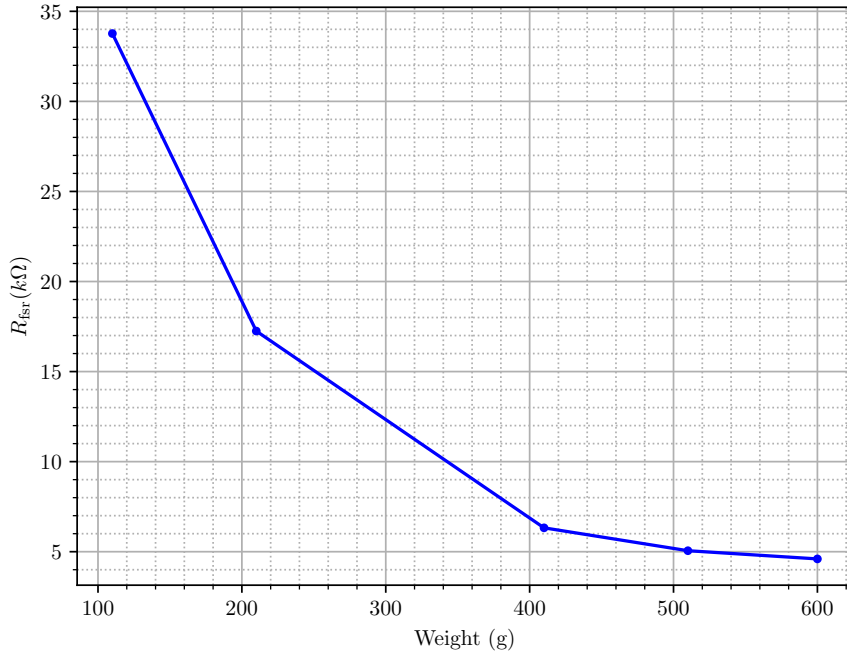


Figure 3.2.3: Calibration of the FSR

3.2.4 Calibration of EMG Sensors

The EMG sensor is used to switch between the flexion and extension states of the device. The value of the sensor reading increases when the muscles are contracted and reduces when the muscles are relaxed. Hence, upon placing the sensors on the flexor muscle group, the higher voltage reading should indicate the device to switch to flexion state and the lower voltage reading should indicate the device to switch to extension state. In order to do this, a threshold needs to be set, beyond which the device will go into the flexion state. Fig. 3.2.4 shows the sensor readings when the electrodes are placed on the flexor group on the anterior forearm. From these readings, it is observed that the flexed state has a higher potential difference than the relaxed state (or the extended state). For this prototype, a value of 100 is chosen to be the lower limit, beyond which the device goes into the flexed state.

We have also measured the EMG signals of the extensor group at the posterior forearm. The readings have been presented in Fig. 3.2.5. Comparing the two muscle groups, the difference between the states is more clearly observed in the flexor group than in the extensor group.

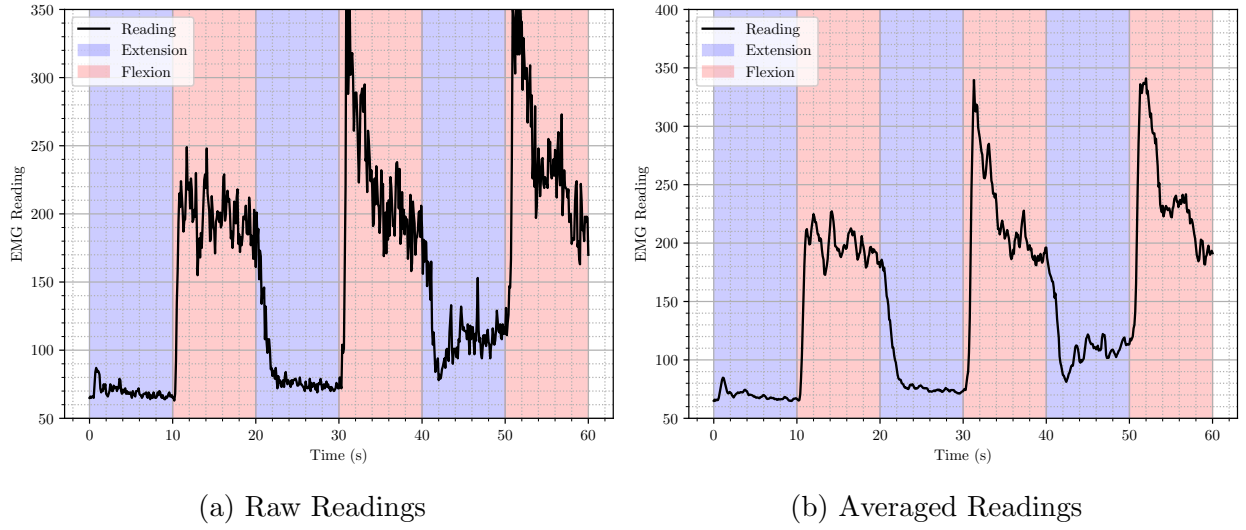


Figure 3.2.4: EMG Sensor Readings: Flexor Group

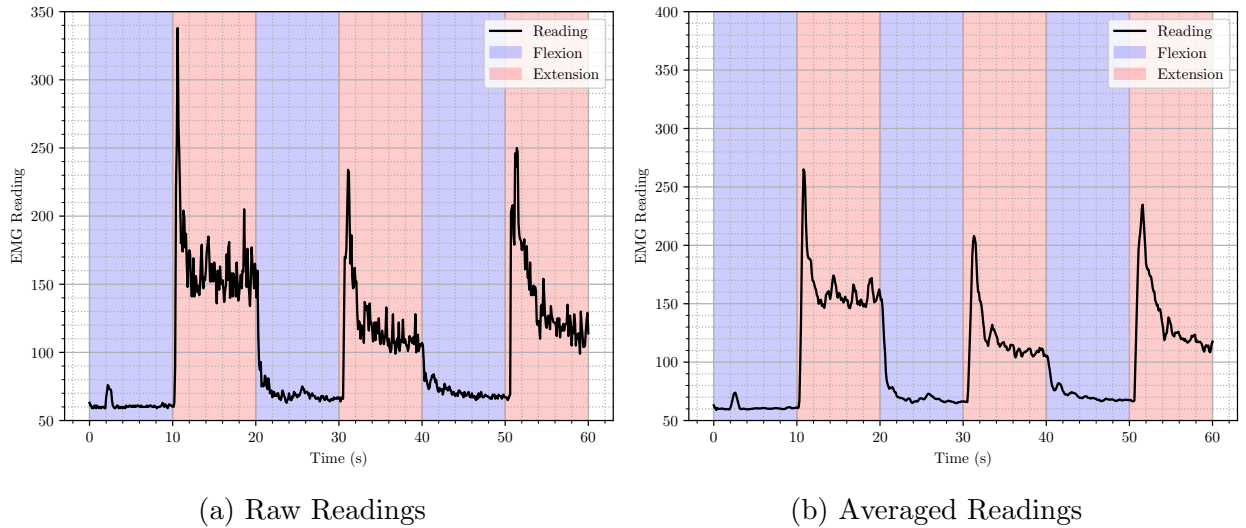
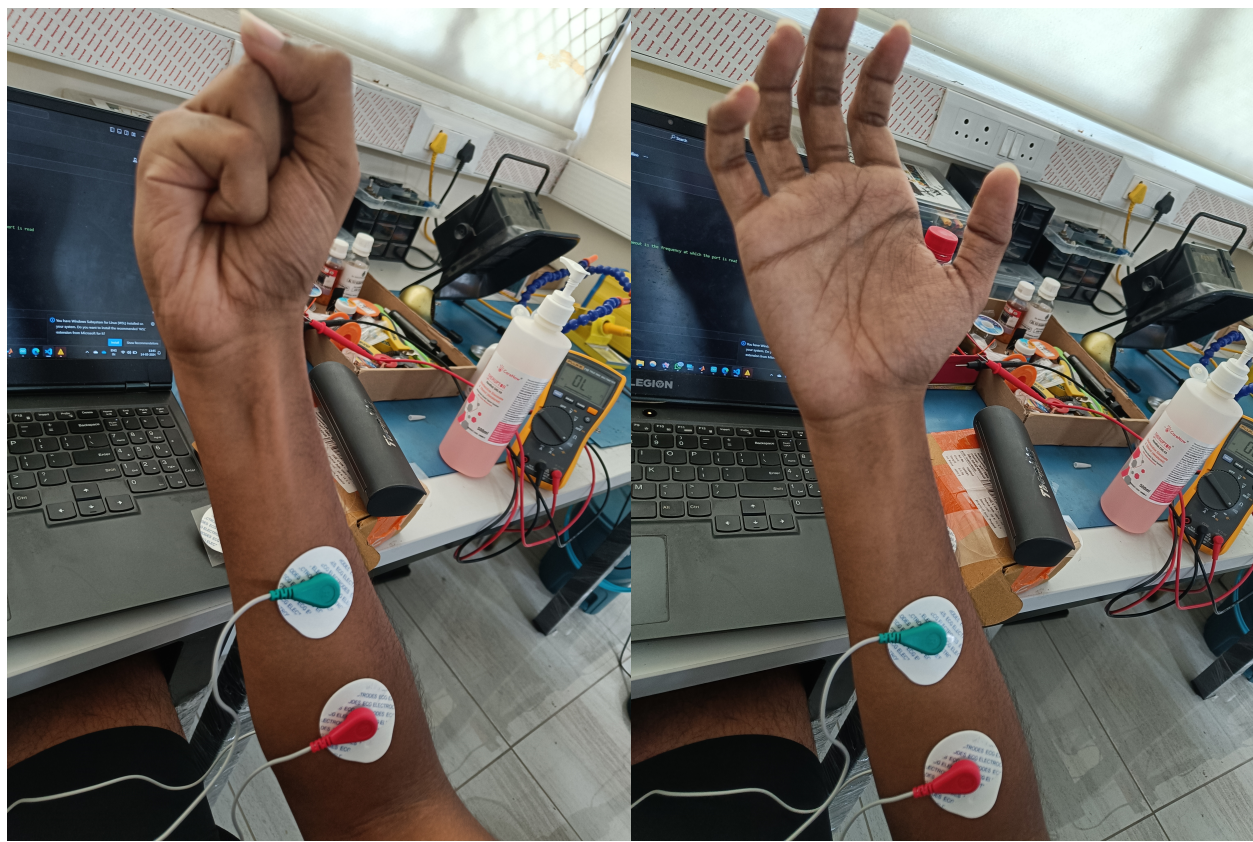


Figure 3.2.5: EMG Sensor Readings: Extensor Group

Thus, we have placed the sensors only on the anterior forearm. The placement of the electrodes and the gestures made during calibration are shown in Fig. ??.

3.2.5 Circuit Diagram

The circuit diagram is presented in Fig. 3.2.9 and 3.2.10. Fig. 3.2.8 mentions the connections of all the components used in the circuit.



(a) Flexed State

(b) Extended State

Figure 3.2.6: Hand gestures and placement of electrodes

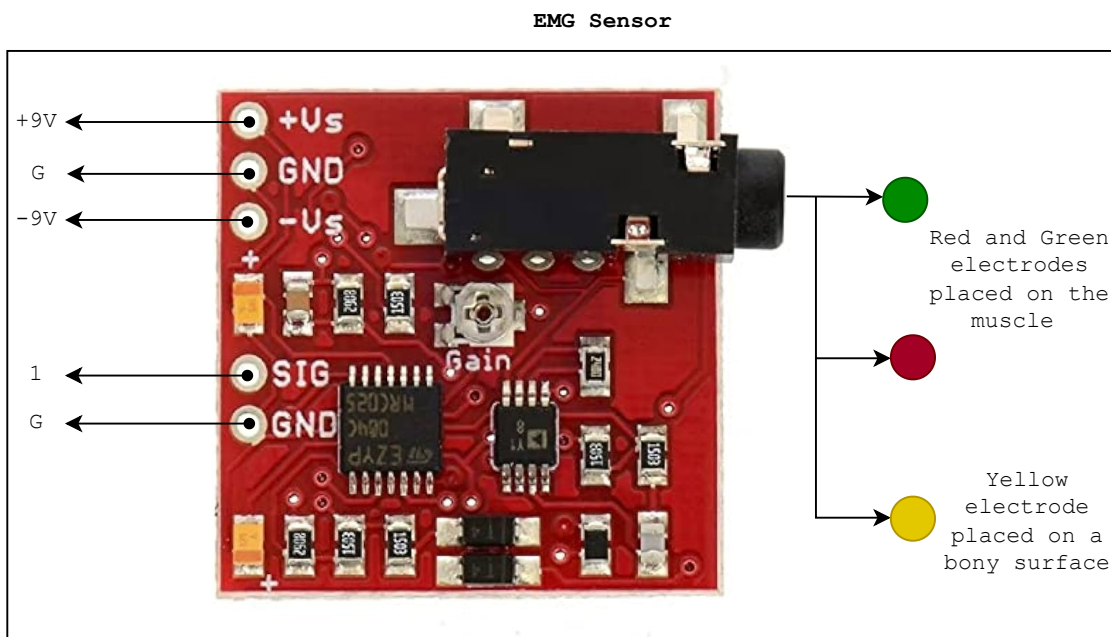
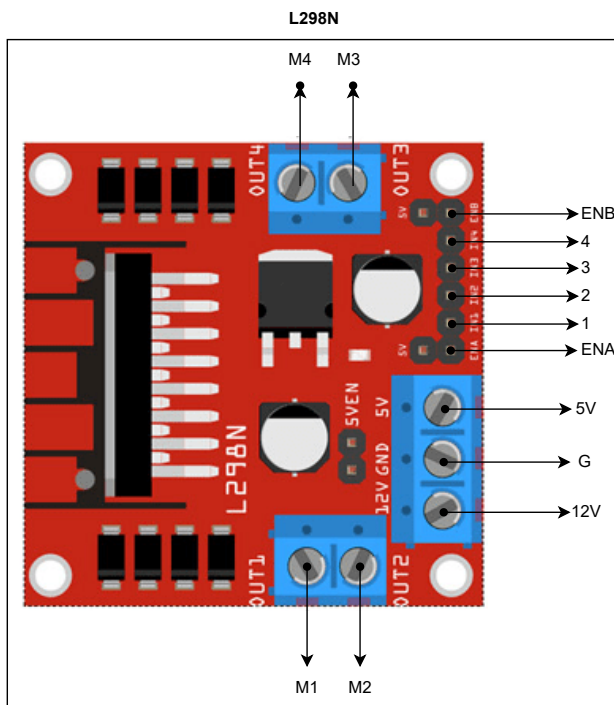
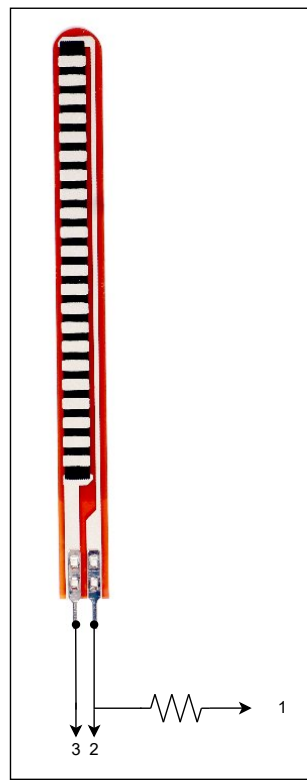


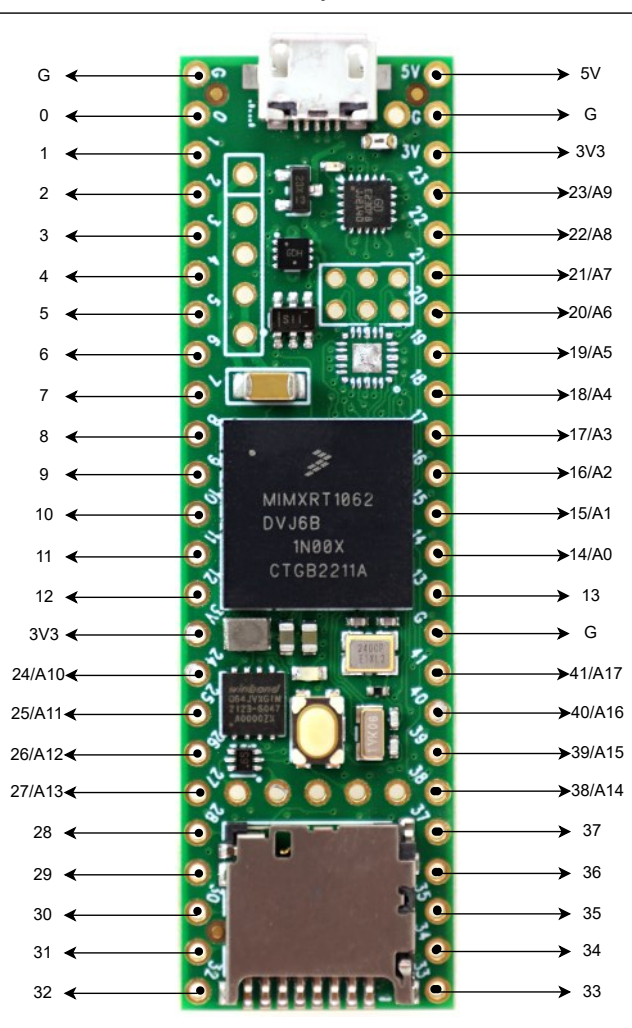
Figure 3.2.7: Components of the circuit



Flex Sensor



Teensy 4.1



Force Sensor



Figure 3.2.8: Components of the circuit continued

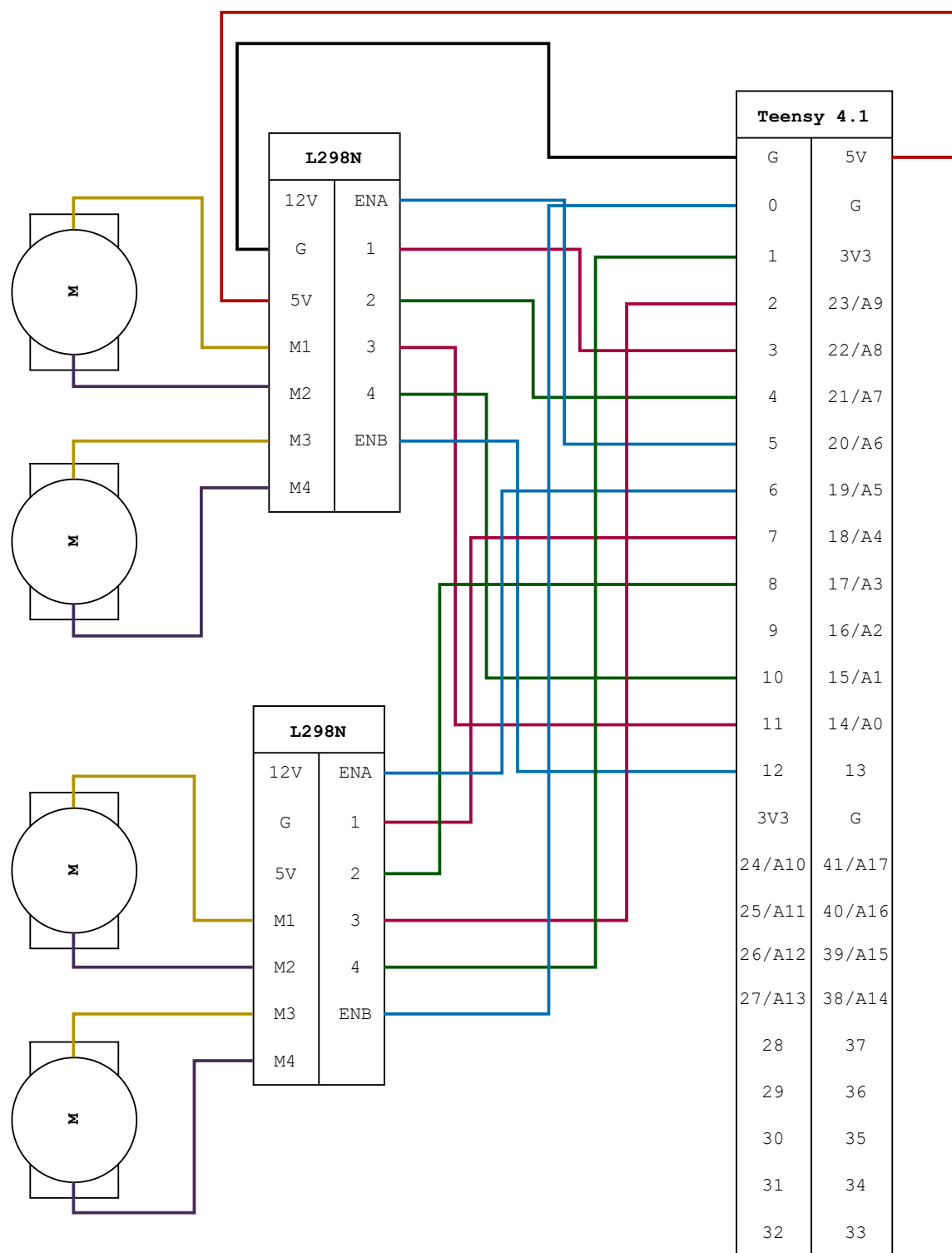


Figure 3.2.9: Circuit Diagram: Actuator Connections

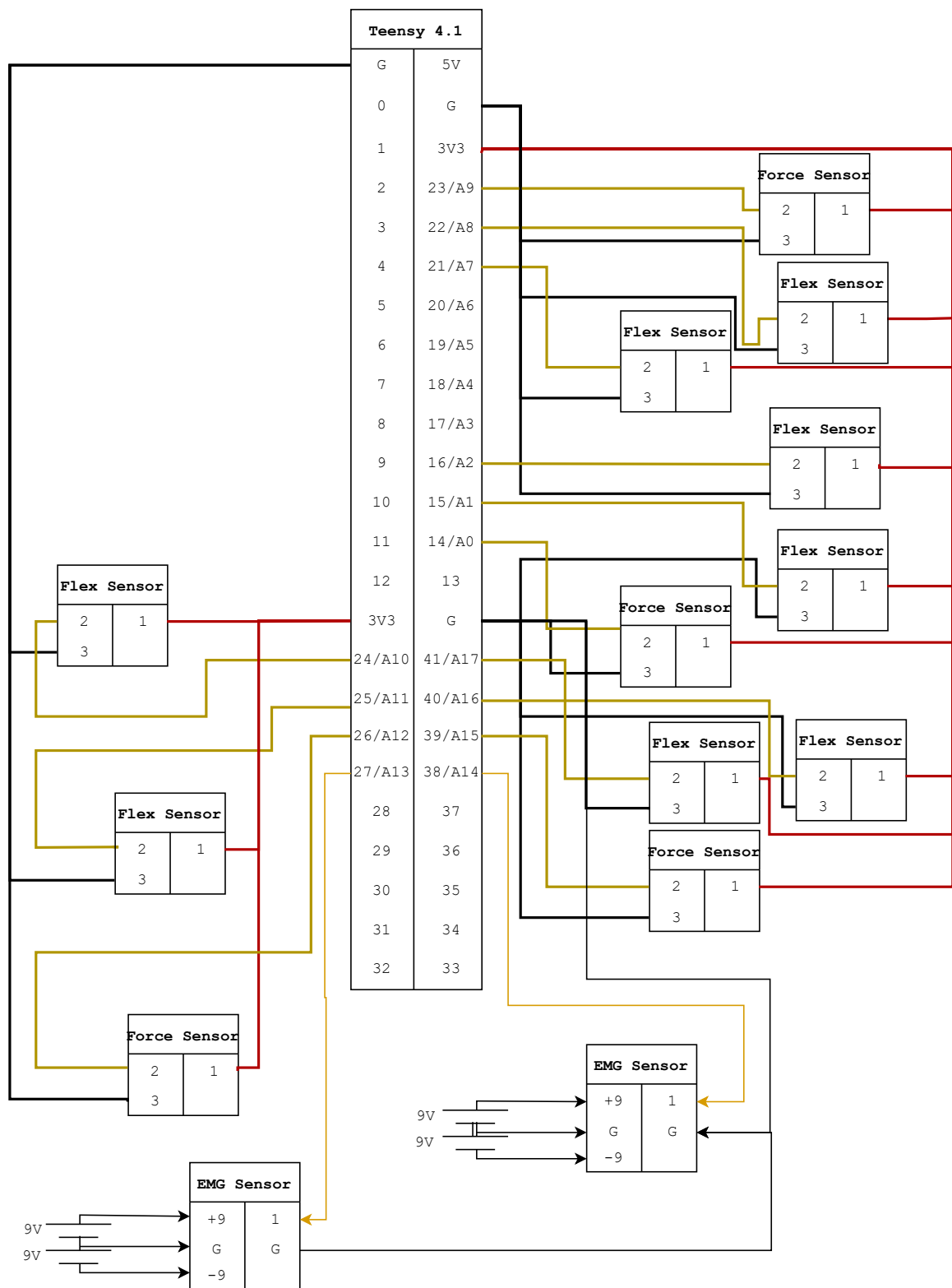


Figure 3.2.10: Circuit Diagram: Sensor Connections

3.3 Placement of the EMG Sensors

As mentioned earlier, the EMG Sensor measures the potential difference between two points in the muscle group that arises when the muscle contracts. In order to ensure accurate readings, it is necessary to place these sensors on or near the muscles that are activated when flexing the fingers of the hand.

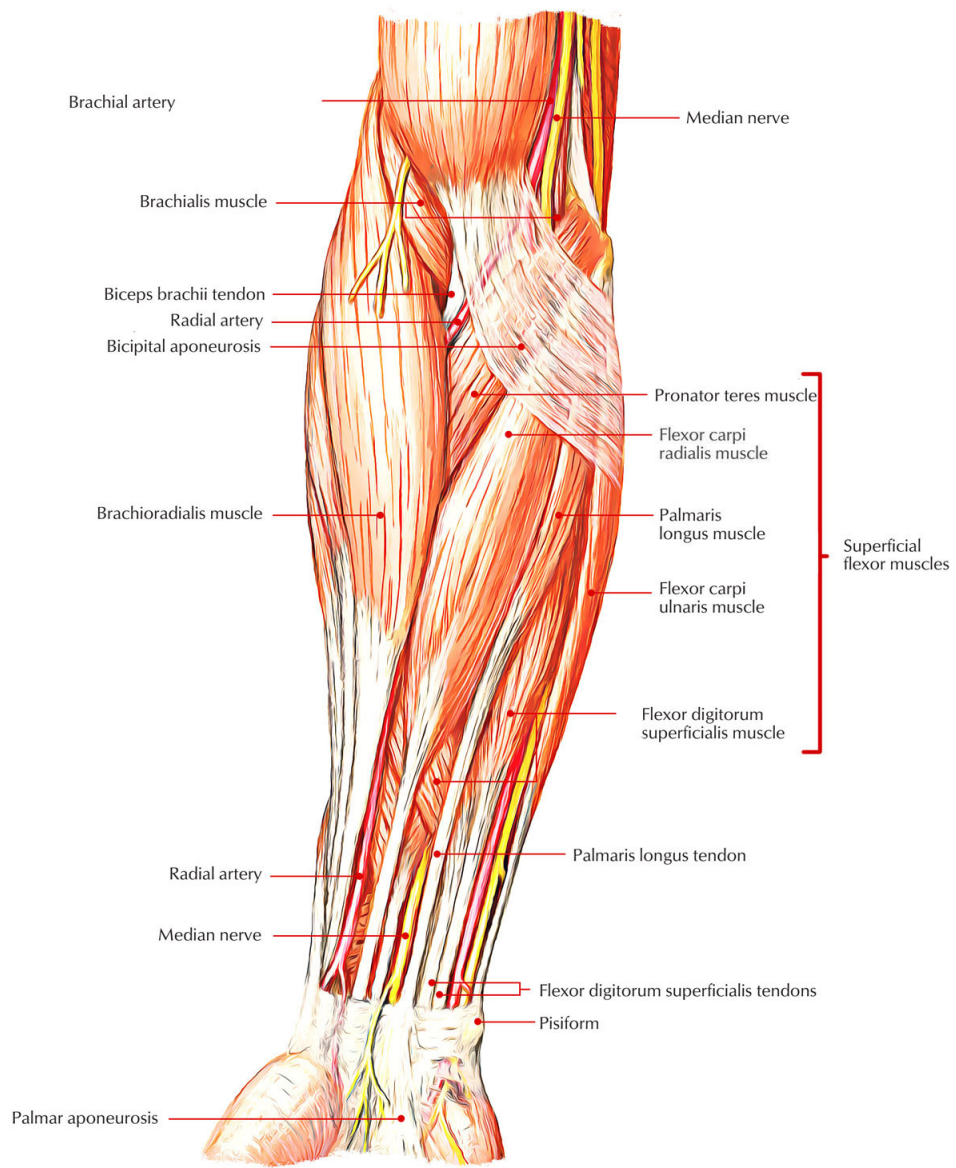


Figure 3.3.1: The Finger Flexor Group
Source: Adapted from [17]

In the human hand, the *flexor digitorum profundus* and the *flexor digitorum superficialis* are primarily responsible for the flexion of the fingers. Both these muscles have their origin in

the forearm. The *flexor digitorum profundus* has its insertion (point of attachment with the bone that the muscle actuates) at the distal phalange, while the *flexor digitorum superficialis* has its insertion at the intermediate phalange [18]. Both these muscles together contract to bring about the flexion motion of the phalanges. The motion of the thumb towards the palm is brought about by the *flexor pollicis longus*. Since all these muscles have their bellies at the anterior forearm region, as shown in Fig. 3.3.1. This would be a good region to place the Flexion EMG sensor, which is used to detect if the user intends to flex their fingers.

The *extensor digitorum* is responsible for the extension of the fingers. Hence, the posterior forearm region would be apt to place the EMG sensor, which is used to detect if the user intends to extend their fingers.

3.4 Control levels

The control levels of this device are broadly divided into three:

1. High-level control - Grasp modes
2. Intermediate control - State machines
3. Low-level control

3.4.1 Grasp modes

This prototype has two grasp modes, enabling the user to perform two different types of actions.

Mode A: Cylindrical grasp Mode A is used to grab a bottle or any similar object. In this mode, the thumb is made to carry out retroposition-opposition, and the other 4 fingers are made to carry out flexion-extension.

Mode B: Lateral pinch Mode B is used to twist open a bottle's cap. In this mode, the thumb is made to carry out abduction-adduction movements, and the rest of the fingers undergo flexion-extension.

With these two modes, we hope to demonstrate that this device indeed makes it easier for people with partial paralysis to carry out these activities. The prototype has one button which can be used to toggle between the two modes of operation.

3.4.2 State machines

When a particular grasp mode is selected, the device goes into the corresponding state machine. A state machine is a representation of how the behavior of the system depends on the inputs it receives from the various sensors present in it. In this device, the sensors used in each mode are:

1. EMG Sensors to detect if the user intends to flex or extend their fingers
2. Force sensors for pinching force measurement
3. Flex sensors for angle measurement

In order to design the state machine, we first define the state variables. These variables typically store some boolean value that is the result of a logical expression containing some combination of the sensor data. For this device, the state variables are defined as follows:

x_1 : Flexion flag

x_2 : Extension flag

x_3 : Value of the force sensor $> 1N$

Assignment of x_1 and x_2 are discussed in Algorithm 1 and Algorithm 2 respectively.

Each state is defined as a unique combination of these state variables. In theory, there can be 16 such states. In this device, however, most of these states are forbidden. The available states are mentioned in Tab. 3.1.

The state machine can also be represented as a flowchart. This representation is called the state machine diagram. Fig. 3.4.1 depicts the state machine diagram for this device.

Algorithm 1: Assignment of Flexion flag (x_1)

Input: EMG_{flex} , θ_{flex} , flex_{th} , flex_{lim}
Output: x_1 flag
Initialize: $x_1 = -1$;
while *true* **do**
 $\text{EMG}_{\text{flex}} = \text{read_EMG_Sensor}();$
 $\theta_{\text{flex}} = \text{read_Flex_Sensor_Angles}();$
 if $\text{EMG}_{\text{flex}} \geq \text{flex}_{\text{th}}$ **then**
 if $\theta_{\text{flex}} \leq \text{flex}_{\text{lim}}$ **then**
 $| x_1 = 1;$
 end
 else
 $| x_1 = 0;$
 end
 end
 else if $x_1 = 1$ *and* $\theta_{\text{flex}} \leq \text{flex}_{\text{lim}}$ **then**
 $| x_1 = 1;$
 end
 else
 $| x_1 = 0;$
 end
end

Algorithm 2: Assignment of Extension flag (x_2)

Input: EMG_{ext} , θ_{ext} , ext_{th} , ext_{lim}
Output: x_2 flag
Initialize: $x_2 = -1$;
while *true* **do**
 $\text{EMG}_{\text{ext}} = \text{read_EMG_Sensor}();$
 $\theta_{\text{ext}} = \text{read_Flex_Sensor_Angles}();$
 if $\text{EMG}_{\text{ext}} \geq \text{ext}_{\text{th}}$ **then**
 if $\theta_{\text{ext}} \geq \text{ext}_{\text{lim}}$ **then**
 $| x_2 = 1;$
 end
 else
 $| x_2 = 0;$
 end
 end
 else if $x_2 = 1$ *and* $\theta_{\text{ext}} \geq \text{ext}_{\text{lim}}$ **then**
 $| x_2 = 1;$
 end
 else
 $| x_2 = 0;$
 end
end

x_1	x_2	x_3	state
0	0	0	idle
0	0	1	idle
0	1	0	extension
0	1	1	extension
1	0	0	flexion
1	0	1	grasp
1	1	0	forbidden
1	1	1	forbidden

Table 3.1: Description of the state machine

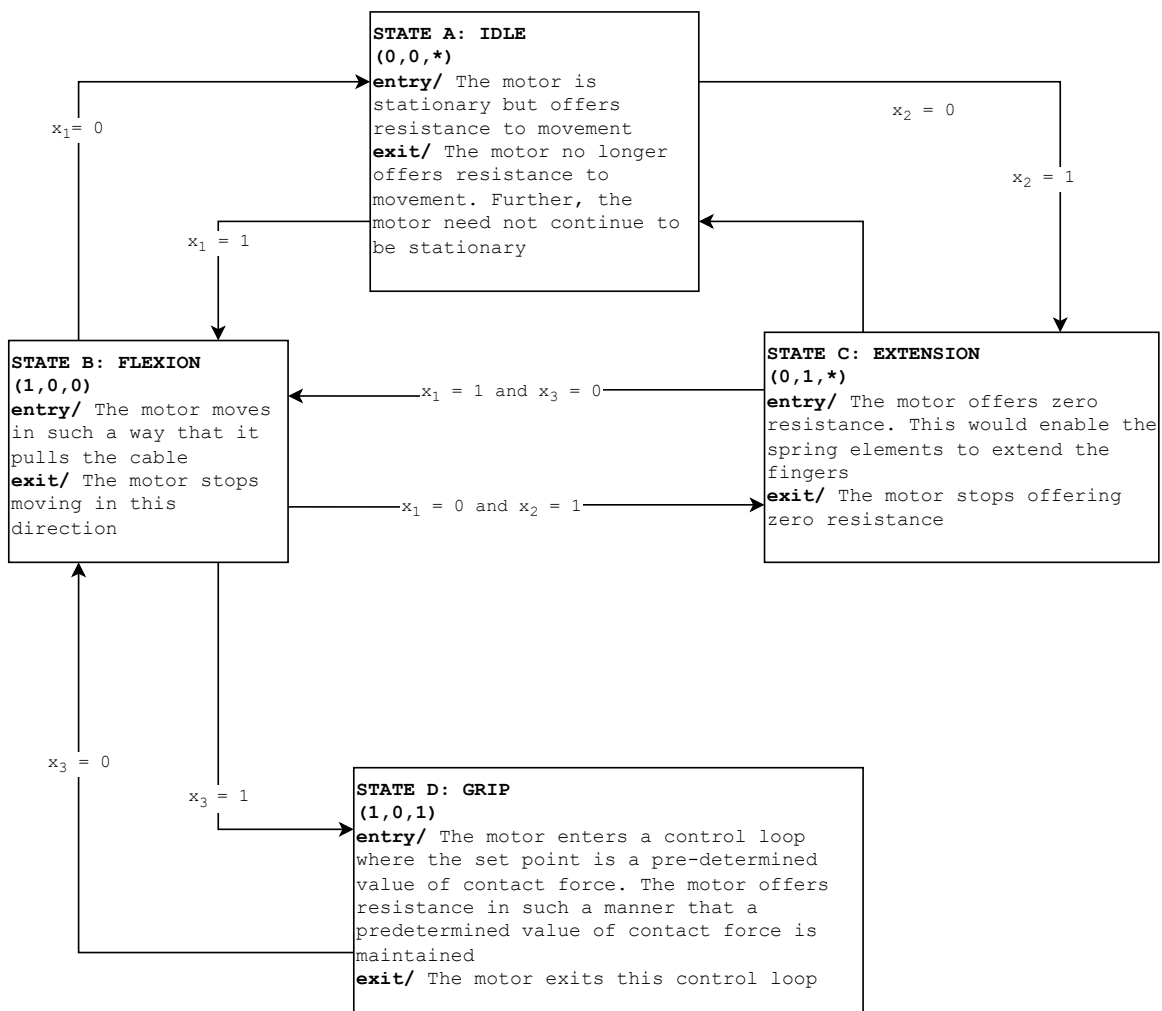


Figure 3.4.1: State Machine Diagram

On the device, this state machine is implemented using switch case statements, coded on the Teensy 4.1 development board using the Arduino IDE. The connections of the sensors to the Teensy are discussed in detail in the next section.

3.4.3 Low-level control

During the extension and flexion states of the device, the motors run at full speed in the respective direction. During the grasp state, the device enters a control loop that ensures a constant pre-defined force is maintained. This is currently a bang-bang controller and can be upgraded to a P or a PID controller once better-quality force sensors are used.

CHAPTER 4

RESULTS AND DISCUSSION

4.1 The prototype

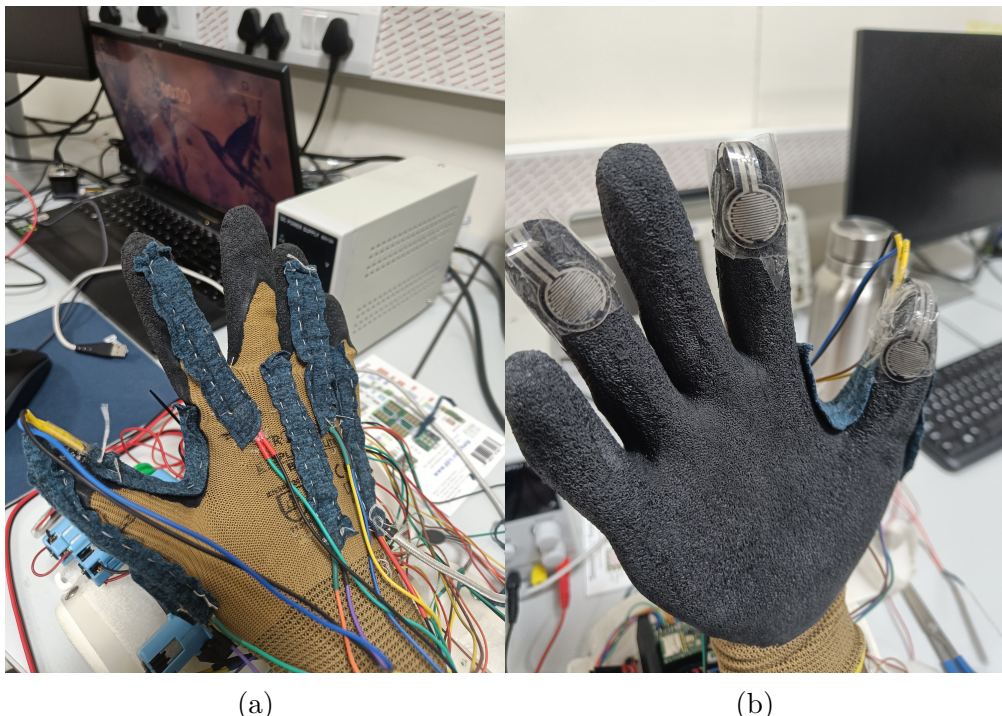
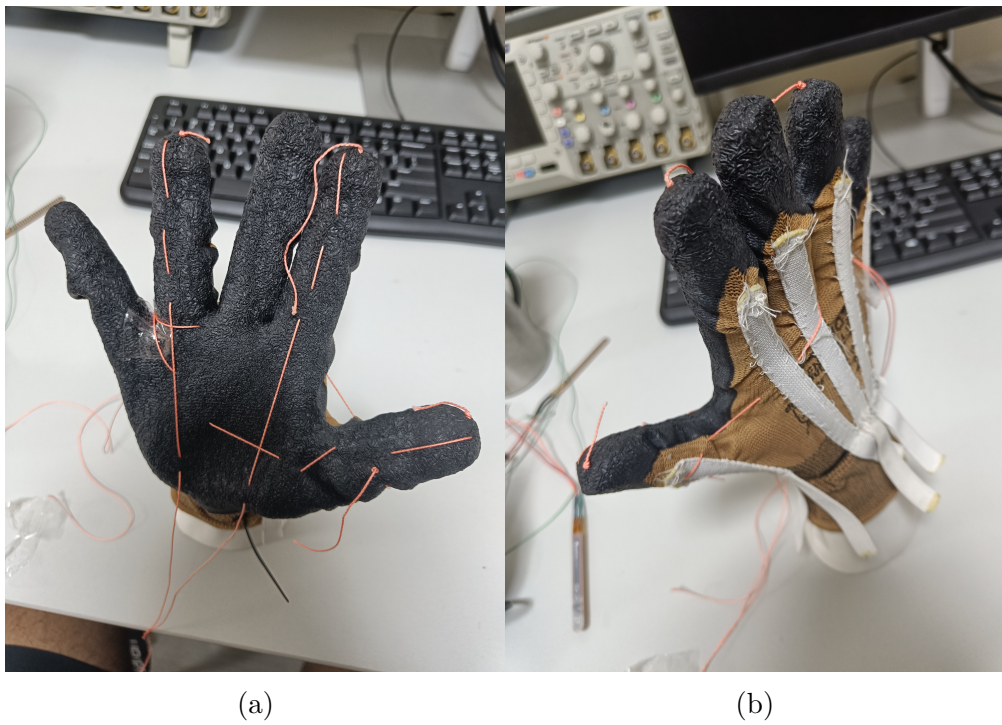


Figure 4.1.1: Sensor glove

In this project, a proof of concept prototype of a wearable hand assistive device has been presented. The device consists of 2 layers: a glove with the flex and force sensors and a glove with the cables and the elastic elements. The gloves are presented in Fig. 4.1.1 and Fig. 4.1.2 respectively. The actuation glove is meant to be donned over the sensor glove, substituting a multi-layered glove.



(a)

(b)

Figure 4.1.2: Actuation glove

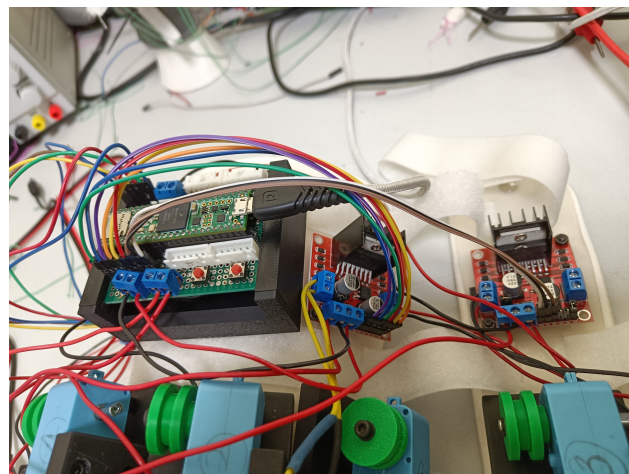


Figure 4.1.3: Control System of the Prototype

The control system is shown in Fig. 4.1.3. The glove attached to the splint is shown in 4.1.4. Fig. 4.1.5 presents a case where the glove was used to grasp an object.

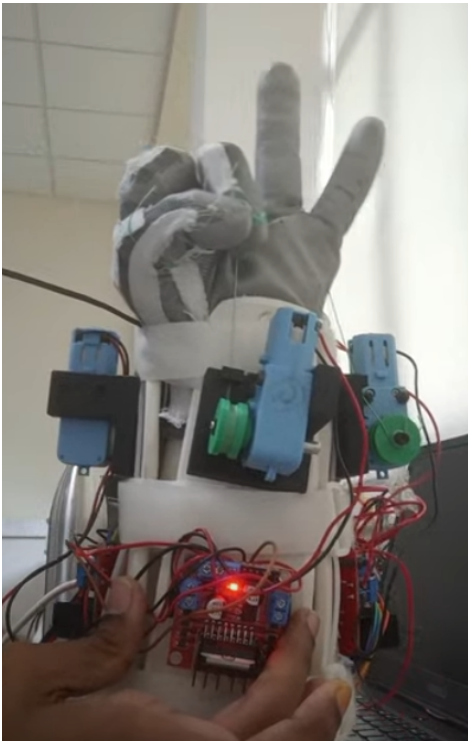


Figure 4.1.4: Glove attached to the splint

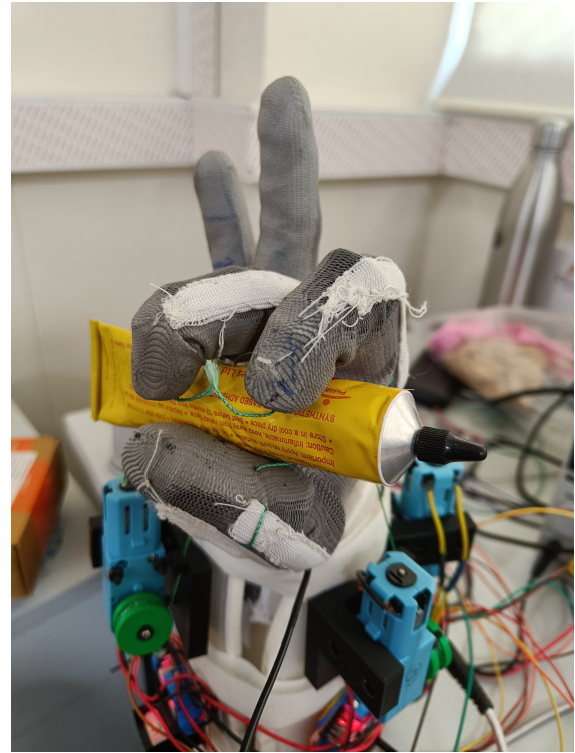


Figure 4.1.5: Grasping a cylindrical object

4.2 Limitations and Future Work

There are a few features of this prototype that can be improved upon. Firstly, the EMG sensors use wet electrodes that have to be stuck to the skin every time the user wears the device. The adhesive layer wears out quickly, leaving this method unsustainable. Currently, most of the weight of the control system is toward the distal end of the arm. It could be relocated to a more proximal end of the arm or could even be housed on the shoulder or hip to reduce the moment arm on the user. Finally, due to space constraints, only three independent compartments could be actuated. This calls for a more efficient solution for housing the actuation system.

With the successful implementation of the POC prototype, our next steps would be aimed at overcoming the limitations stated in the previous paragraph. Firstly, we intend to make the EMG sensor-based intent detection much more robust by employing a wearable high-density EMG band. Then, we aim to work towards finding a more seamless way to incorporate the actuators into the fabric of the device to reduce the bulk. The usage of micro-motors is one potential avenue to explore.

Bibliography

- [1] R. Singh, “Epidemiology of spinal cord injuries: Indian perspective,” *Epidemiology of Spinal Cord Injuries*, pp. 157–168, Sep. 2012.
- [2] P. Brown, D. Jones, S. Singh, and J. Rosen, “The exoskeleton glove for control of paralyzed hands,” en, in [1993] *Proceedings IEEE International Conference on Robotics and Automation*, Atlanta, GA, USA: IEEE Comput. Soc. Press, 1993, pp. 642–647, ISBN: 978-0-8186-3450-5. DOI: [10.1109/ROBOT.1993.292051](https://doi.org/10.1109/ROBOT.1993.292051). [Online]. Available: <http://ieeexplore.ieee.org/document/292051/> (visited on 05/01/2024).
- [3] M. F. Rotella, K. E. Reuther, C. L. Hofmann, E. B. Hage, and B. F. BuSha, “An orthotic hand-assistive exoskeleton for actuated pinch and grasp,” en, in *2009 IEEE 35th Annual Northeast Bioengineering Conference*, Cambridge, MA, USA: IEEE, Apr. 2009, pp. 1–2, ISBN: 978-1-4244-4362-8. DOI: [10.1109/NEBC.2009.4967693](https://doi.org/10.1109/NEBC.2009.4967693). [Online]. Available: <http://ieeexplore.ieee.org/document/4967693/> (visited on 05/01/2024).
- [4] L. A. Martinez, O. O. Olaloye, M. V. Talarico, S. M. Shah, R. J. Arends, and B. F. BuSha, “A power-assisted exoskeleton optimized for pinching and grasping motions,” en, in *Proceedings of the 2010 IEEE 36th Annual Northeast Bioengineering Conference (NEBEC)*, New York, NY, USA: IEEE, Mar. 2010, pp. 1–2, ISBN: 978-1-4244-6879-9. DOI: [10.1109/NEBEC.2010.5458232](https://doi.org/10.1109/NEBEC.2010.5458232). [Online]. Available: <http://ieeexplore.ieee.org/document/5458232/> (visited on 05/01/2024).
- [5] P. Polygerinos, K. C. Galloway, E. Savage, M. Herman, K. O. Donnell, and C. J. Walsh, “Soft robotic glove for hand rehabilitation and task specific training,” en, in *2015 IEEE International Conference on Robotics and Automation (ICRA)*, Seattle, WA, USA: IEEE, May 2015, pp. 2913–2919, ISBN: 978-1-4799-6923-4. DOI: [10.1109/ICRA.2015.7139597](https://doi.org/10.1109/ICRA.2015.7139597). [Online]. Available: <http://ieeexplore.ieee.org/document/7139597/> (visited on 05/01/2024).
- [6] H. K. Yap, B. W. K. Ang, J. H. Lim, J. C. H. Goh, and C.-H. Yeow, “A fabric-regulated soft robotic glove with user intent detection using EMG and RFID for hand assistive application,” in *2016 IEEE International Conference on Robotics and Automation (ICRA)*, May 2016, pp. 3537–3542. DOI: [10.1109/ICRA.2016.7487535](https://doi.org/10.1109/ICRA.2016.7487535). [Online]. Available: <https://ieeexplore.ieee.org/abstract/document/7487535> (visited on 05/01/2024).
- [7] H. K. Yap, J. H. Lim, F. Nasrallah, and C.-H. Yeow, “Design and Preliminary Feasibility Study of a Soft Robotic Glove for Hand Function Assistance in Stroke Survivors,” English, *Frontiers in Neuroscience*, vol. 11, Oct. 2017, Publisher: Frontiers, ISSN: 1662-453X. DOI: [10.3389/fnins.2017.00547](https://doi.org/10.3389/fnins.2017.00547). [Online]. Available: <https://www.frontiersin.org/journals/neuroscience/articles/10.3389/fnins.2017.00547/full> (visited on 05/01/2024).

- [8] HyunKi In, Kyu-Jin Cho, KyuRi Kim, and BumSuk Lee, “Jointless structure and under-actuation mechanism for compact hand exoskeleton,” en, in *2011 IEEE International Conference on Rehabilitation Robotics*, Zurich: IEEE, Jun. 2011, pp. 1–6, ISBN: 978-1-4244-9862-8 978-1-4244-9863-5 978-1-4244-9861-1. DOI: [10.1109/ICORR.2011.5975394](https://doi.org/10.1109/ICORR.2011.5975394). [Online]. Available: <http://ieeexplore.ieee.org/document/5975394/> (visited on 05/01/2024).
- [9] M. Xiloyannis, L. Cappello, Dinh Binh Khanh, Shih-Cheng Yen, and L. Masia, “Modelling and design of a synergy-based actuator for a tendon-driven soft robotic glove,” en, in *2016 6th IEEE International Conference on Biomedical Robotics and Biomechatronics (BioRob)*, Singapore, Singapore: IEEE, Jun. 2016, pp. 1213–1219, ISBN: 978-1-5090-3287-7. DOI: [10.1109/BIOROB.2016.7523796](https://doi.org/10.1109/BIOROB.2016.7523796). [Online]. Available: <http://ieeexplore.ieee.org/document/7523796/> (visited on 05/01/2024).
- [10] L. Gerez, J. Chen, and M. Liarokapis, “On the Development of Adaptive, Tendon-Driven, Wearable Exo-Gloves for Grasping Capabilities Enhancement,” en, *IEEE Robotics and Automation Letters*, vol. 4, no. 2, pp. 422–429, Apr. 2019, ISSN: 2377-3766, 2377-3774. DOI: [10.1109/LRA.2019.2890853](https://doi.org/10.1109/LRA.2019.2890853). [Online]. Available: <https://ieeexplore.ieee.org/document/8601355/> (visited on 05/01/2024).
- [11] X. Chen, L. Gong, L. Wei, *et al.*, “A Wearable Hand Rehabilitation System With Soft Gloves,” *IEEE Transactions on Industrial Informatics*, vol. 17, no. 2, pp. 943–952, Feb. 2021, Conference Name: IEEE Transactions on Industrial Informatics, ISSN: 1941-0050. DOI: [10.1109/TII.2020.3010369](https://doi.org/10.1109/TII.2020.3010369). [Online]. Available: <https://ieeexplore.ieee.org/abstract/document/9146885> (visited on 05/01/2024).
- [12] M. Ciocarlic and J. Stein, “Wearable and functional hand orthotic,” en, US20190060099A1, Feb. 2019. [Online]. Available: [https://patents.google.com/patent/US20190060099A1/en?q=\(wearable+flexion+initiation+glove\)&oq=wearable+flexion+initiation+glove](https://patents.google.com/patent/US20190060099A1/en?q=(wearable+flexion+initiation+glove)&oq=wearable+flexion+initiation+glove) (visited on 05/01/2024).
- [13] N. BUGTAI, A. P. ONG, M. MANGUERRA, *et al.*, “Device for hand rehabilitation,” en, WO2020226518A1, Nov. 2020. [Online]. Available: [https://patents.google.com/patent/WO2020226518A1/en?q=\(wearable+flexion+initiation+glove\)&oq=wearable+flexion+initiation+glove](https://patents.google.com/patent/WO2020226518A1/en?q=(wearable+flexion+initiation+glove)&oq=wearable+flexion+initiation+glove) (visited on 05/01/2024).
- [14] A. Rahman and A. Al-Jumaily, “Design and Development of a Bilateral Therapeutic Hand Device for Stroke Rehabilitation,” *International Journal of Advanced Robotic Systems*, vol. 10, no. 12, p. 405, Dec. 2013, Publisher: SAGE Publications, ISSN: 1729-8806. DOI: [10.5772/56809](https://doi.org/10.5772/56809). [Online]. Available: <https://doi.org/10.5772/56809> (visited on 05/19/2024).
- [15] I. The MathWorks, *Simulink*, version R2023a, 2024. [Online]. Available: <https://www.mathworks.com/products/simulink.html>.
- [16] G. B. Langford, “Flexible potentiometer,” US5583476A, Dec. 1996. [Online]. Available: <https://patents.google.com/patent/US5583476A/en> (visited on 04/25/2024).
- [17] *Muscles of the Anterior or Front of the Forearm*, en-US, Aug. 2018. [Online]. Available: <https://www.earthslab.com/anatomy/muscles-anterior-front-forearm/> (visited on 05/05/2024).
- [18] J. D. Nguyen and H. Duong, “Anatomy, Shoulder and Upper Limb, Hand Long Flexor Tendons and Sheaths,” eng, in *StatPearls*, Treasure Island (FL): StatPearls Publishing, 2024. [Online]. Available: <http://www.ncbi.nlm.nih.gov/books/NBK546607/> (visited on 05/02/2024).